J. Appl. Comput. Mech., 11(2) (2025) 485-501
DOI: 10.22055/jacm.2024.46976.4637

ISSN: 2383-4536
jacm.scu.ac.ir

Shahid Chamran University of Ahvaz

Journal of Applied and Computational Mechanics

Research Paper

Modeling and Numerical Simulations of Fuzzy-Fractional Oldroyd 6-Constant Nanofluid

Mubashir Qayyum[1], Aneeza Tahir[1], Syed Tauseef Saeed[2]

[1] Department of Sciences and Humanities, National University of Computer and Emerging Sciences, Lahore, 54770, Pakistan,
Email: mubashir.qayyum@nu.edu.pk (M.Q.); l217946@lhr.nu.edu.pk (A.T.)

[2] Department of Mathematics and Statistics, The University of Lahore, Lahore, 54590, Pakistan,
Email: tauseef.saeed@math.uol.edu.pk

Received May 21 2024; Revised August 17 2024; Accepted for publication August 29 2024.
Corresponding author: S.T. Saeed (tauseef.saeed@math.uol.edu.pk)

Abstract. This article contains analysis of thin film flow of fuzzy-fractional Oldroyd-6 constant nanofluid in lift and drain cases. The fluid has ability to model both viscous and elastic behaviors accurately in different complex flow regimes and geometries. Due to these features, this fluid is very important in food cosmetics industries. Typically, the variables in these models are assumed to have crisp values regardless of uncertainties or memory effects in the phenomena. To incorporate uncertainty in the current modeling, triangular fuzzy numbers (TFNs) are used in the boundary conditions and volume fraction of nanoparticle along with a consideration of Caputo derivative. We examine effects of obtained fuzzy numbers for more accurate and realistic analysis of flow regime. To further improve the model accuracy, fuzzy based numerical methods are used to solve the obtained system, which helps in precise quantification of uncertainty associated with each parameter. Furthermore, effect of different parameters on the velocity profiles is analyzed numerically and graphically. The validation and convergence of the obtained solutions are checked by capturing residual errors in each case. Analysis reveals that in draining case, increase in material parameter ζ_1 leads to a less pronounced and more diffuse fuzzy velocity profile. On the other hand, increase in material parameter ζ_2 and gravitational parameter g_r amplifies the fuzzy velocity field, indicating a stronger and faster flow; however, opposite behavior is observed in lifting case. The end result of this modeling is more accurate and realistic portrayal of nanofluidic flow, which reflects the complexities of phenomena more closely.

Keywords: Oldroyd 6-Constatnt model; Nanofluid; Caputo derivative; Fuzzy modeling; Homotopy perturbation.

1. Introduction

In practice, it is well understood that Newtonian fluids cannot accurately model the behavior of viscoelasticity and polymer solutions of the phenomena. The classical Navier–Stokes (NS) equations are inadequate for modeling the rheological behavior of viscoelastic fluids and polymer solutions, which occurs in variety of engineering and biological systems. This has made it necessary to modify the NS equations and develop new models that are capable of capturing the rheological properties of complex fluids more accurately. Among many, Oldroyd 6-constant fluid is of special interest due to its ability to model viscoelastic fluids in wide range of situations. Therefore, over the time, many new models have been developed and broadly classified into rate-type [1], differential-type [2], and n-type fluids [3]. In simple configurations like those involving unidirectional steady flows, the Oldroyd-B (3-constant) model can be used which includes variables like fluid velocity, stress, time derivatives, viscosity, retardation and relaxation, and rate of strain [4-7]. However, when it comes to complex configurations such as those involving instabilities or multidimensional problems, more sophisticated models such as the Oldroyd-C (6-constant) and Oldroyd-D (8-constant) models are required [8-11].

The Oldroyd 6-constant model is widely used to model the behavior of viscoelastic fluids. These fluids include polymer solutions, liquid crystals, and biological fluids, and production of plastics and paint. Baris [12] examined the steady and slow two-dimensional flow of an Oldroyd 6-constant fluid between moving and fixed intersecting planes. Wang et al. [13] created a mathematical model for predicting the velocity profile of an incompressible, unidirectional flow of an electrically conducting Oldroyd 6-constant fluid under the influence of a transverse magnetic field. The effectiveness of optimal homotopy asymptotic method (OHAM) for solving non-linear differential equations of non-Newtonian fluids is studied by Manzoor et al. in [14]. He focused on the Oldroyd 6-constant fluid with slippage and analyzed its behavior in three types of flow problems known as plane Couette flow, generalized Couette flow, and plane Poiseuille flow. Rana et al. [15] conducted a numerical investigation of the hydromagnetic flow between two concentric cylinders using an incompressible Oldroyd 6-constant fluid. Qayyum and Fatima [16] did numerical analysis of thin film flows of Pseudo-Plastic and Oldroyd 6-constant fluids. Bhatti and Michaelides [17] studied Oldroyd

Published online: September 11 2024

6-constants fluid in parallel micro-plates with heat transfer. Salawu and Disu [18] investigated the behavior of a reactive flow in Oldroyd 6-constant fluid. Moreover, the work is also further extended in fractional space. The homotopic solutions of fractional thin film of Oldroyd 6-constant are studied by Farnaz et al. [19].

The world we live-in is a complex place, and its complexity is often attributed to uncertainty and ambiguity. Fuzzy set theory is a useful tool for modeling real-world problems that involve incomplete information about the variables and parameters [20]. Mathematical equations can be used to create models of dynamical real-life problems, which can take the form of ordinary or partial differential equations. When information about the behavior of dynamical system is inadequate, fuzzy differential equations are valuable modeling tools. In situations where ordinary measurement is not sufficient to detect fuzzy parameters associated with uncertain or inconsistent phenomena, fuzzy differential equations with fuzzy initial conditions may be used. Such equations provide suitable mathematical models for many real-life applications like population models [21], physics [22], and medicine [23]. To mathematically handle such situations, different fuzzy numbers are available in literature including triangular, exponential, Gaussian, and trapezoidal fuzzy numbers. Nadeem et al. [24] utilized triangular fuzzy numbers (TFNs) to analyzed the impact of MHD and gravitational parameters on a third-grade fluid. Qayyum et al. [25, 26] proposed and utilized fuzzy extension of He–Laplace algorithm to Fractional-Fuzzy Fisher models. Khaliq et al. [27] investigated fuzzy model of tumor growth patterns by utilizing the generalized Hukuhara derivative. Naeem et al. [28] utilized the iterative method with Laplace transform along with Caputo-Fabrizio operator to analyze fractional-fuzzy Korteweg-De Vries equation. Hoa et al. [29] studied different fuzzy-fractional differential equations using Caputo-Katugampola fractional derivative. Rashid et al. [30] investigated fuzzy-fractional Boussinesq model in oceanography. The recent investigations on various aspects of fuzzy differential models can be seen in [31-34].

The objective of current study is to model and simulate fuzzy-fractional Oldroyd 6-constant nanofluid. This study utilizes a fuzzification approach that relies on triangular fuzzy numbers (TFNs) including α-cut to indicate the degree of membership within a given interval. By doing so, the approach facilitates a more precise representation of uncertainty in a model to make it more realistic depiction of industrial and biological processes characterized by uncertain data. Specifically, the study puts forward several numerical and semi-numerical algorithms for fuzzy-fractional analysis of Oldroyd 6-constant nanofluid. The article is structured into several sections. In Section 2, the preliminary concept of the current study is introduced. The methodology of the proposed approach is outlined in Section 3, while its convergence analysis is presented in Section 4. Section 5 depicts a mathematical description of the problem using fuzzy logic. The findings and analysis are presented in Section 6 through graphical and tabular representations. Finally, Section 7 concludes the article with some concluding remarks.

2. Preliminaries

Definition I: A fuzzy number $\tilde{T}$ is itself a fuzzy set which satisfies following conditions [35]:

- $\tilde{T}$ is upper semi-continuous.
- $\tilde{T}(y)=0$ outside the interval $[g,h]$.
- There exist a real number $e,f: g\le e\le f\le h$ for which:
  $\tilde{T}(y)=1$, when $e\le y\le f$.
  $\tilde{T}(y)$ is monotonically increasing on $[g,e]$ and monotonically decreasing on $[f,h]$.

Definition II [35]: A fuzzy number $\tilde{T}$ is defined as a pair of functions $(\underline{T},\overline{T})$ that meets the following requirements for $0\le\alpha\le 1$.

- $\underline{T}(\alpha)$ is bounded, monotonic increasing, and left-continuous function.
- $\overline{T}(\alpha)$ is bounded, monotonic decreasing, and left-continuous function.
- $\underline{T}(\alpha)$ is less than or equal to $\overline{T}(\alpha)$.

Definition III [36]: Assume that the fuzzy number $\tilde{T}=(s_1,s_2,s_3)$ is known to be a triangular fuzzy number (TFN) if:

$$\mu_{\tilde{T}}(y)=\begin{cases}0, & \text{if } y\le s_1\\ \dfrac{y-S_1}{S_2-S_1}, & \text{if } s_1\le y\le s_2\\ \dfrac{S_3-y}{S_2-S_1}, & \text{if } s_2\le y\le s_3\\ 0, & \text{if } y\ge s_3\end{cases}. \tag{1}$$

Definition IV [37]: The α level set of a fuzzy number $\tilde{T}$ is given as:

$$[\tilde{T}]^{\alpha}=\{y\,|\,\mu_{\tilde{T}}(y)\ge\alpha\},\quad 0\le\alpha\le 1, \tag{2}$$

where the $\tilde{T}=(s_1,s_2,s_3)$ is implied, with the following $\alpha-$cut:

$$\tilde{T}=[\underline{T}(y;\alpha),\overline{T}(y;\alpha)]=[s_1+(s_2-s_1)\alpha, s_3-(s_3-s_2)\alpha].$$

Definition V [38]: The fractional derivative of fuzzy valued function $\tilde{T}$ of order β in the Caputo sense is given by:

$$D_k^{\beta}\tilde{T}(k)=\begin{cases}\dfrac{1}{\Gamma(\eta-\beta)}\displaystyle\int_0^k(k-p)^{\eta-\beta-1}\dfrac{d^{\beta}\tilde{T}(p)}{dp^{\beta}}, & \text{if } \eta-1<\beta<\eta\\ \dfrac{d^{\beta}\tilde{T}(p)}{dp^{\beta}}, & \text{otherwise } \beta=\eta\end{cases}. \tag{3}$$

Definition VI [38]: The Laplace transform associated with Caputo's fractional derivative (3), can be formulated as follows:

$$L[D_k^{\beta}\tilde{T}(k)]=s^{\beta}L[\tilde{T}(k)]-\sum_{j=0}^{\eta-1}s^{\beta-j-1}\tilde{T}^{\eta}(0),\qquad \eta-1<\beta<\eta. \tag{4}$$

3. Methodology of Fuzzy He-Laplace Algorithm

We have examined a non-linear time fractional ordinary differential equation in order to illustrate the fundamental concept behind this approach. The equation is expressed as follows:

$$\left[D_x^{\beta}\tilde{F}(x)\right]_{\alpha}+\left[\mathfrak{A}\tilde{F}(x)\right]_{\alpha}+\left[\mathfrak{R}\tilde{F}(x)\right]_{\alpha}=\left[f(x)\right]_{\alpha},\qquad \beta>0,\ \ \eta-1<\beta\le\eta, \tag{5}$$

where α is a value between 0 and 1 that defines a level set. Consider a known function $f(x)$ an unknown function $\tilde{F}(x)$ and linear and non-linear operators denoted by $\mathfrak{A}$ and $\mathfrak{R}$, respectively. The equation above can be expressed in interval form by utilizing the $\alpha-$cut:

$$\begin{aligned}
&\left[\tilde{F}(x)\right]_{\alpha}=\underline{F}(x;\alpha),\overline{F}(x;\alpha)\\
&\left[D_x^{\beta}\tilde{F}(x)\right]_{\alpha}=D_x^{\beta}\underline{F}(x;\alpha),D_x^{\beta}\overline{F}(x;\alpha)\\
&\left[\mathfrak{A}\tilde{F}(x)\right]_{\alpha}=\mathfrak{A}\underline{F}(x;\alpha),\mathfrak{A}\overline{F}(x;\alpha)\\
&\left[\mathfrak{R}\tilde{F}(x)\right]_{\alpha}=\mathfrak{R}\underline{F}(x;\alpha),\mathfrak{R}\overline{F}(x;\alpha)\\
&\left[f(x)\right]_{\alpha}=\underline{f}(x;\alpha),\overline{f}(x;\alpha)
\end{aligned}$$

Equation (5) can also be written as:

$$\left[D_x^{\beta}\underline{F}(x;\alpha),D_x^{\beta}\overline{F}(x;\alpha)\right]+\left[\mathfrak{A}\underline{F}(x;\alpha),\mathfrak{A}\overline{F}(x;\alpha)\right]+\left[\mathfrak{R}\underline{F}(x;\alpha),\mathfrak{R}\overline{F}(x;\alpha)\right]=\left[\underline{f}(x;\alpha),\overline{f}(x;\alpha)\right]. \tag{6}$$

By applying the differential property of Laplace transform (4), the aforementioned equation is converted to:

$$L\left[\underline{F}(x;\alpha),\overline{F}(x;\alpha)\right]-\frac{1}{s^{\beta}}\sum_{w=0}^{\eta-1}s^{\beta-w-1}\tilde{F}^{(\eta)}(0)+\frac{1}{s^{\beta}}L\left\{\left[\mathfrak{A}\underline{F}(x;\alpha),\mathfrak{A}\overline{F}(x;\alpha)\right]+\left[\mathfrak{R}\underline{F}(x;\alpha),\mathfrak{R}\overline{F}(x;\alpha)\right]-\left[\underline{f}(x;\alpha),\overline{f}(x;\alpha)\right]\right\}=0. \tag{7}$$

The homotopy of Eq. (7) is:

$$\begin{aligned}
&(1-\wp)\left\{L\left[\underline{F}(x;\alpha),\overline{F}(x;\alpha)\right]-L\left[\underline{F}_0(x;\alpha),\overline{F}_0(x;\alpha)\right]\right\}\\
&+\wp\left[L\left[\underline{F}(x;\alpha),\overline{F}(x;\alpha)\right]-\frac{1}{s^{\beta}}\sum_{w=0}^{\eta-1}s^{\beta-w-1}\left[\underline{F}^{(\eta)}(0;\alpha),\overline{F}^{(\eta)}(0;\alpha)\right]+\frac{1}{s^{\beta}}L\left\{\left[\mathfrak{A}\underline{F}(x;\alpha),\mathfrak{A}\overline{F}(x;\alpha)\right]+\left[\mathfrak{R}\underline{F}(x;\alpha),\mathfrak{R}\overline{F}(x;\alpha)\right]-\left[\underline{f}(x;\alpha),\overline{f}(x;\alpha)\right]\right\}\right]=0,
\end{aligned} \tag{8}$$

where $F_0(x;\alpha)$ is the initial guess. Now expanding $\tilde{F}_{x;\alpha}$ in terms of a Taylor series with respect to $\wp$ for lower and upper bound:

$$\tilde{F}(x;\alpha)=\left[\underline{F}(x;\alpha),\overline{F}(x;\alpha)\right]\sum_{w=1}^{\infty}\wp^{w}\tilde{F}_w. \tag{9}$$

After substituting the aforementioned equation into the homotopy equation, and equating the coefficients of with the same powers.

We obtain the following equations at first and second order, respectively:

$$L\left\{\tilde{F}_1(x;\alpha)\right\}+\tilde{F}_2(x;\alpha)-\frac{1}{s^{\beta}}\sum_{w=0}^{\eta-1}s^{\beta-w-1}\tilde{F}^{(\eta)}(0)+\frac{1}{s^{\beta}}L\left\{\left[\mathfrak{A}\tilde{F}_0(x;\alpha)\right]+\left[\mathfrak{R}\tilde{F}_0(x;\alpha)\right]-\left[\tilde{f}(x;\alpha)\right]\right\}=0,\ \tilde{F}_1^{(\eta)}(0)=\Im_1^{\eta}, \tag{10}$$

$$L\left\{\tilde{F}_2(x;\alpha)\right\}+\tilde{F}_1(x;\alpha)-\frac{1}{s^{\beta}}\sum_{w=0}^{\eta-1}s^{\beta-w-1}\tilde{F}^{(\eta)}(0)+\frac{1}{s^{\beta}}L\left\{\left[\mathfrak{A}\tilde{F}_1(x;\alpha)\right]+\left[\mathfrak{R}\tilde{F}_1(x;\alpha)\right]-\left[\tilde{f}(x;\alpha)\right]\right\}=0,\ \tilde{F}_2^{(\eta)}(0)=\Im_2^{\eta}. \tag{11}$$

Generally, j-th order equation can be written as:

$$L\left\{\tilde{F}_j(x;\alpha)\right\}+\frac{1}{s^{\beta}}L\left\{\left[\mathfrak{A}\tilde{F}_{j-1}(x;\alpha)\right]+\left[\mathfrak{R}\tilde{F}_{j-1}(x;\alpha)\right]\right\}=0,\ \tilde{F}_{j-1}^{(\eta)}(0)=\Im_{j-1}^{\eta}, \tag{12}$$

and inverse Laplace transformation of the j-th order equation is:

$$\tilde{F}_j(x;\alpha)+L^{-1}\left\{\frac{1}{s^{\beta}}L\left\{\left[\mathfrak{A}\tilde{F}_{j-1}(x;\alpha)\right]+\left[\mathfrak{R}\tilde{F}_{j-1}(x;\alpha)\right]\right\}\right\}=0. \tag{13}$$

The final expression for the approximate solution of a general fractional fuzzy ordinary differential equation is given by:

$$\tilde{F}=\tilde{F}_0(x;\alpha)+\tilde{F}_1(x;\alpha)+\tilde{F}_2(x;\alpha)+\tilde{F}_3(x;\alpha)+\ldots\ldots \tag{14}$$

4. Convergence Analysis

4.1. Convergence Theorem

Consider the two functions $\tilde{F}_n(x;\alpha)$ and $\tilde{F}(x;\alpha)$ defined in a Banach space $\left(\mathrm{B}[0,T],\|.\|\right)$. Then the series solution in Eq. (14) converges to solution of Eq. (5), whenever $\gamma\in(0,1)$.

Proof: Suppose for the sequence of partial sum of series (14), we need to show that $\tilde{z}_n(x;\alpha)$ is a Cauchy sequence in Banach space $\left(\mathrm{B}[0,T],\|.\|\right)$. For this, we let:

$$
\begin{aligned}
\left\|\tilde{z}_{n+1}(x;\alpha)-\tilde{z}_{n}(x;\alpha)\right\| &= \left\|\tilde{F}_{n+1}(x;\alpha)\right\| \\
&\leq \gamma\left\|\tilde{F}_{n}(x;\alpha)\right\| \\
&\leq \gamma^{2}\left\|\tilde{F}_{n-1}(x;\alpha)\right\| \leq \dots \leq \gamma^{n+1}\left\|\tilde{F}_{0}(x;\alpha)\right\|.
\end{aligned} \tag{15}
$$

Now, for every $n,m \in \mathrm{N}$, $n \geq m$, there exist two arbitrary sums $\tilde{z}_n$ and $\tilde{z}_m$ by successively applying triangular inequality, we get:

$$
\begin{aligned}
\left\|\tilde{z}_{n}-\tilde{z}_{m}\right\| &= \left\|\left(\tilde{z}_{n}(x;\alpha)-\tilde{z}_{n-1}(x;\alpha)\right)+\left(\tilde{z}_{n-1}(x;\alpha)-\tilde{z}_{n-2}(x;\alpha)\right)+\dots+\left(\tilde{z}_{m+1}(x;\alpha)-\tilde{z}_{m}(x;\alpha)\right)\right\| \\
&\leq \left\|\left(\tilde{z}_{n}(x;\alpha)-\tilde{z}_{n-1}(x;\alpha)\right)\right\|+\left\|+\left(\tilde{z}_{n-1}(x;\alpha)-\tilde{z}_{n-2}(x;\alpha)\right)\right\|+\dots+\left\|\left(\tilde{z}_{m+1}(x;\alpha)-\tilde{z}_{m}(x;\alpha)\right)\right\|.
\end{aligned} \tag{16}
$$

Using Eq. (15), we get:

$$
\begin{aligned}
\left\|\tilde{z}_{n}-\tilde{z}_{m}\right\| &\leq \gamma^{n}\left\|\tilde{F}_{0}(x;\alpha)\right\|+\gamma^{n-1}\left\|\tilde{F}_{0}(x;\alpha)\right\|+\dots+\gamma^{m+1}\left\|\tilde{F}_{0}(x;\alpha)\right\| \\
&\leq \left(\gamma^{n}+\gamma^{n-1}+\dots..+\gamma^{m+1}\right)\left\|\tilde{F}_{0}(x;\alpha)\right\| \\
&\leq \gamma^{m+1}\left(\gamma^{n-m-1}+\gamma^{n-m-2}+\dots..+\gamma+1\right)\left\|\tilde{F}_{0}(x;\alpha)\right\| \\
&\leq \gamma^{m+1}\left(\frac{1-\gamma^{n-m}}{1-\gamma}\right)\left\|\tilde{F}_{0}(x;\alpha)\right\|.
\end{aligned} \tag{17}
$$

Given $0<\gamma<1$, we have $1-\gamma^{n-m}<1$. Thus:

$$
\left\|\tilde{z}_{n}-\tilde{z}_{m}\right\| \leq \left(\frac{\gamma^{m+1}}{1-\gamma}\right)\max_{t\in[0,T]}\left|\tilde{F}_{0}(x;\alpha)\right|. \tag{18}
$$

Since it is bounded, it yields:

$$
\lim_{n,m\to\infty}\left\|\tilde{z}_{n}(x;\alpha)-\tilde{z}_{m}(x;\alpha)\right\|=0.
$$

Therefore, sequence $\{\tilde{z}_n\}$ is a Cauchy sequence in Banach space B and hence is convergent.

5. Mathematical Formulation and Simulation of Fuzzy-Fractional Thin Film of Oldroyd 6-Constant Nanofluid

5.1. Governing Equations

The equation of motion for an incompressible fluid, while ignoring thermal effects can be expressed as:

$$
\operatorname{div} \mathrm{V} = 0, \tag{19}
$$

$$
\rho\left[(\mathrm{V}.\nabla)\mathrm{V}+\frac{\partial \mathrm{V}}{\partial t}\right] = \nabla.\mathrm{T}+\rho \mathrm{z}, \tag{20}
$$

where t is the time, ρ is the fluid's density, ρz represents the body forces per unit mass and V represents the velocity vector.

The Cauchy stress tensor T is defined as:

$$
\mathrm{T}=\mathrm{S}-p\mathrm{N}. \tag{21}
$$

Hence, N represents the unit tensor, p is the pressure and S is extra stress tensor which is given as:

$$
\mathrm{S} = \left[\mu+\nu\left|\sqrt{\frac{1}{2}\operatorname{tr}(\mathrm{R}_1)}\right|^{k-1}\right]\mathrm{R}_1, \tag{22}
$$

where the constants u,v,k are defined differently for different fluids, while R_1 represents the rate of deformation tensor:

$$
\mathrm{S}+\gamma_1\frac{DS}{Dt}+\frac{\gamma_3}{2}(\mathrm{S}\mathrm{R}_1+\mathrm{R}_1\mathrm{S})+\frac{\gamma_5}{2}(tr\,\mathrm{S})\mathrm{R}_1=\mu(\mathrm{R}_1+\gamma_2\frac{D\mathrm{R}_1}{Dt}+\gamma_4\mathrm{R}_1^2) \tag{23}
$$

$$
\mathrm{R}_1=L+L^T,\ L=grad\,V. \tag{24}
$$

Here, $\mu,\gamma_1,\gamma_2,\gamma_3,\gamma_4$ and γ_5 are the material constant while R_1 represents the Rivlin Ericksen tensor. The contravariant convected derivative is given by:

$$
\frac{D(.)}{Dt}=\frac{d(.)}{dt}-L(.)-(.)L^T, \tag{25}
$$

where $\frac{d(.)}{dt}$ denotes the material derivative.

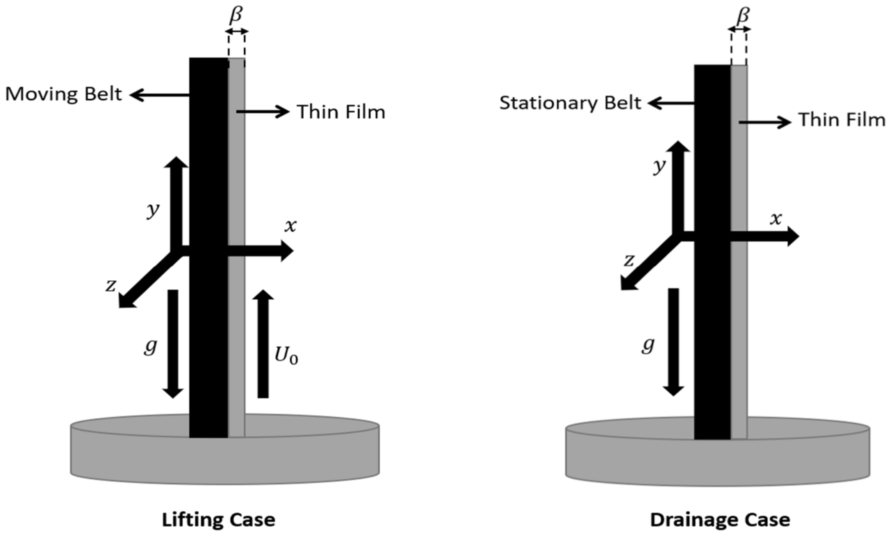

Fig. 1. Schematic configuration of the flow structure.

5.2. Mathematical Modeling of Oldroyd 6-Constant Nanofluid in Lifting Scenario

We examine a container that contains an in-compressible non-Newtonian nanofluid. A wide belt moves vertically upwards through the container at a constant speed of U_0, taking up a thin layer of fluid that has a uniform thickness β. The fluid is affected by gravity, causing it to drain down the belt. For the sake of simplicity, we assume that the fluid flow is uniform, steady, and laminar, and that the thickness of the fluid film is uniform throughout.

To establish a coordinate system, we select an $xy-$ plane, with the $x-$ axis parallel to the fluid and perpendicular to the belt, the $y-$ axis upwards along the belt, and the $z-$ axis normal to the $xy-$ plane. As the only velocity component present is in the $y-$ direction. The flow geometry of the problem is presented in Fig. 1. As the only velocity component present is in the $y-$ direction. Thus:

$$V = \left(0, F(x), 0\right), \tag{26}$$

and S is a function of x only. i.e.,

$$S = S(x). \tag{27}$$

Putting Eqs. (21), (26) and (27) in Eq. (20), we get:

$$\frac{\partial p}{\partial x} = \frac{dS_{xx}}{dx}, \tag{28}$$

$$\frac{\partial p}{\partial y} = \frac{dS_{yx}}{dx} + pg_y, \tag{29}$$

$$\frac{\partial p}{\partial z} = \frac{dS_{zx}}{dx}. \tag{30}$$

Inserting Eqs. (26) and (27) in Eqs. (24) and (25), we get:

$$S_{xx} + \gamma_3 S_{yx}\frac{dF}{dx} = \mu\gamma_4\left(\frac{dF}{dx}\right)^2, \tag{31}$$

$$S_{xy} - \gamma_1 S_{xx}\frac{dF}{dx} + \frac{\gamma_3+\gamma_5}{2}\left(S_{xx}+S_{yy}\right)\frac{dF}{dx} = \mu\gamma_4\frac{dF}{dx}, \tag{32}$$

$$S_{xz} + \frac{\gamma_3}{2}S_{yz}\frac{dF}{dx} = 0, \tag{33}$$

$$S_{yy} - [2\gamma_1 - \gamma_3]S_{xy}\frac{dF}{dx} = \mu[\gamma_4 - 2\gamma_2]\left(\frac{dF}{dx}\right)^2, \tag{34}$$

$$S_{yz} - \left[\gamma_1 - \frac{\gamma_3}{2}\right]S_{xz}\frac{dF}{dx} = 0. \tag{35}$$

From Eqs. (33) and (35), we get:

$$S_{xz} = S_{yz} = 0. \tag{36}$$

Now, by adding Eqs. (31) and (34), we have:

$$S_{xx} + S_{yy} = [2\gamma_1 - \gamma_3]S_{xy}\frac{dF}{dx} + \mu[\gamma_4 - 2\gamma_2]\left(\frac{dF}{dx}\right)^2, \tag{37}$$

$$S_{xy} = \frac{\mu}{1+\zeta_2\left(\frac{dF}{dx}\right)^2}\left[\frac{dF}{dx} + \zeta_1\left(\frac{dF}{dx}\right)^3\right]. \tag{38}$$

Here, the constants ζ_1 and ζ_2 are defined as:

$$\zeta_1 = \gamma_1\gamma_2 - (\gamma_3+\gamma_5)(\gamma_4-\gamma_2),$$

$$\zeta_2 = \gamma_1\gamma_3 - (\gamma_3+\gamma_5)(\gamma_3-\gamma_1).$$

From Eqs. (28), (29), (30) and (36), we obtain:

$$\frac{\partial p}{\partial z} = 0.$$

Taking $\hat{p} = p - S_{xx}$, we get:

$$\frac{\partial \hat{p}}{\partial z} = \frac{\partial \hat{p}}{\partial x} = 0.$$

This equation implies that pressure is solely a function of y. Thus, Eq. (29) takes the following form:

$$\frac{\partial \hat{p}}{\partial z} = pg_y + \frac{dS_{yx}}{dx}. \tag{39}$$

As there is no pressure gradient along $y-$direction, this constant can be taken to be zero and fluid is going upward. Using Eq. (38) in (39), the final governing equation for the flow of an Oldroyd 6-constant nanofluid is given by:

$$\frac{\partial^2 F}{\partial x^2} + [3\zeta_1 - \zeta_2]\left(\frac{dF}{dx}\right)^2\frac{\partial^2 F}{\partial x^2} + \zeta_1\zeta_2\left(\frac{dF}{dx}\right)^4\frac{\partial^2 F}{\partial x^2} - \frac{\rho_{nf}}{\mu_{nf}}\left[1+\zeta_2\left(\frac{dF}{dx}\right)^2\right]^2 = 0. \tag{40}$$

Now using boundary condition $S_{xy} = 0$ at $x = \beta$ in Eq. (38), we get $dF/dx = 0$ at $x = \beta$. Hence:

$$\begin{aligned} &F = U_0 \quad \text{at} \quad x = 0, \\ &\frac{dF}{dx} = 0 \quad \text{at} \quad x = \beta. \end{aligned} \tag{41}$$

To non-dimensionalize form of Eq. (40) subject to Eq. (41), we introduced the dimensionless parameters as:

$$v^* = \frac{v}{U_0}, x^* = \frac{x}{\beta}, \gamma_1^* = \frac{\gamma_1}{\left(\beta/U_0\right)^2}, \gamma_2^* = \frac{\gamma_2}{\left(\beta/U_0\right)^2}, g_r^* = \frac{\rho_f g\beta^2}{\mu_f U_0}, D_1 = \frac{\rho_{nf}}{\rho_f}, D_2 = \frac{\mu_{nf}}{\mu_f}.$$

From Eq. (40), we have:

$$\frac{\partial^2 F}{\partial x^2} + [3\zeta_1 - \zeta_2]\left(\frac{dF}{dx}\right)^2\frac{\partial^2 F}{\partial x^2} + \zeta_1\zeta_2\left(\frac{dF}{dx}\right)^4\frac{\partial^2 F}{\partial x^2} - \frac{D_1}{D_2}g_r\left[1+\zeta_2\left(\frac{dF}{dx}\right)^2\right]^2 = 0. \tag{42}$$

with,

$$\begin{aligned} &F(x) = 1 \quad \text{at} \quad x = 0, \\ &\frac{dF}{dx} = 0 \quad \text{at} \quad x = 1. \end{aligned} \tag{43}$$

5.3. Fuzzification of Fractional Oldroyd 6-Constant Nanofluid in Lifting Case

To incorporate a degree of fuzziness into the model, we added it to both the nanoparticles' volume fraction parameter and the boundary conditions. To accomplish this, we introduced triangular fuzzy numbers and discretized them using (h_1,h_2,h_3) and (w_1,w_2,w_3) as fuzzy parameters for the $\alpha-$cut. For instance, we can take the volume fraction of nanoparticles (η), within the range of $[0.01-0.05]$, and represent it as a triangular fuzzy number with the values $\eta = (0.001, 0.03, 0.05)$. This allows us to account for the inherent uncertainties and variations in the system, which can significantly impact its behavior and performance. By utilizing these fuzzy numbers, we can modify Eq. (42) to incorporate the degree of fuzziness:

$$\left[\frac{d^{\beta}(\underline{F})}{dx^{\beta}},\frac{d^{\beta}(\overline{F})}{dx^{\beta}}\right]+[3\zeta_1-\zeta_2]\left[\left(\frac{d(\underline{F})}{dx}\right)^2,\left(\frac{d(\overline{F})}{dx}\right)^2\right]\left[\frac{d^{\beta}(\underline{F})}{dx^{\beta}},\frac{d^{\beta}(\overline{F})}{dx^{\beta}}\right]+\zeta_1\zeta_2\left[\left(\frac{d(\underline{F})}{dx}\right)^4,\left(\frac{d(\overline{F})}{dx}\right)^4\right]\left[\frac{d^{\beta}(\underline{F})}{dx^{\beta}},\frac{d^{\beta}(\overline{F})}{dx^{\beta}}\right]-\frac{D_1}{D_2}g_r\left(1+\zeta_2\left[\left(\frac{d(\underline{F})}{dx}\right)^2,\left(\frac{d(\overline{F})}{dx}\right)^2\right]\right)^2=0. \tag{44}$$

Here, $D_1=(1-\eta)+\eta(\rho_s/\rho_f)$, $D_2=1/(1-\eta)^{2.5}$, where η presents the volume fraction with Fuzzy condition:

$$\begin{aligned}\tilde{F}(x;\alpha)&=\left[\underline{F}(x;\alpha),\overline{F}(x;\alpha)\right]=\tilde{A}=\left[h_1+(h_2-h_1)\alpha,h_3-(h_3-h_2)\alpha\right],\text{ at } x=0,\\ \frac{d\tilde{F}(x;\alpha)}{dx}&=\left[\frac{d\underline{F}(x;\alpha)}{dx},\frac{d\overline{F}(x;\alpha)}{dx}\right]=\tilde{B}=\left[w_1+(w_2-w_1)\alpha,w_3-(w_3-w_2)\alpha\right],\text{ at } x=1.\end{aligned} \tag{45}$$

where the TFNs $\tilde{A}=(0.2,1,1.1),\tilde{B}=(-0.001,0,0.001)$, and $\eta=(0.001,0.03,0.05)$ have $\alpha-$cut expressed as $[0.8\alpha+0.2,1.1-0.1\alpha]$, $[0.001(\alpha-1),0.001(1-\alpha)]$, and $[0.001+0.029\alpha,0.05-0.02\alpha]$, respectively.

5.4. Solution of Fuzzy-Fractional Model in Lifting Case

We can expend $\underline{F}$ and $\overline{F}$ in Taylor series form as:

$$\underline{F}=\sum_{i=0}^{\infty}p^i\underline{F}_i, \tag{46}$$

$$\overline{F}=\sum_{i=0}^{\infty}p^i\overline{F}_i, \tag{47}$$

where, $\underline{F}_i,\overline{F}_i$ corresponds to the ith-order lower and upper deformation velocity profiles. Putting fractional order $\beta=2$ along with Eqs. (46) and (47) in Eq. (44) and compare the coefficients of like powers of p gives the following deformation equations:

0th-order fuzzy problem and solution:

$$\begin{aligned}&\underline{F}_0''(x)=0,\ \underline{F}_0(0)=0.2+0.8\alpha,\ \underline{F}_0'(1)=0.001\alpha-0.001,\\ &\underline{F}_0(x;\alpha)=0.2+0.8\alpha+(-0.001+0.001\alpha)x.\end{aligned} \tag{48}$$

$$\begin{aligned}&\overline{F}_0''(x)=0,\ \overline{F}_0(0)=1.1-0.1\alpha,\ \overline{F}_0'(1)=0.001-0.001\alpha,\\ &\overline{F}_0(x;\alpha)=1.1-0.1\alpha+(0.001-0.001\alpha)x.\end{aligned} \tag{49}$$

1st-order fuzzy problem and solution:

$$-\frac{D_1}{D_2}g_r(1+2\varsigma_2\underline{F}_0'(x)^2+\varsigma_2^2\underline{F}_0'(x)^4)+(3\varsigma_1-\varsigma_2)\underline{F}_0'(x)^2\underline{F}_0''(x)+\varsigma_1\varsigma_2\underline{F}_0'(x)^4\underline{F}_0''(x)+\underline{F}_1''(x)=0,\quad \underline{F}_0(0)=0,\quad \underline{F}_0'(1)=0, \tag{50}$$

$$\begin{aligned}\underline{F}_1(x;\alpha)=&\frac{1}{2}g_r(0.999-0.029\alpha)^{2.5}(1.01653+0.479356\alpha)x\times\left(-2+x-4\times10^{-6}(1-1.\alpha)^2\zeta_2+2(0.001-0.001\alpha)^2x\zeta_2\right.\\ &\left.-2\times10^{-12}(1-1.\alpha)^4\zeta_2^2+\zeta_2^2(0.001-0.001\alpha)^4x\right).\end{aligned} \tag{51}$$

$$-\frac{D_1}{D_2}g_r(1+2\varsigma_2\overline{F}_0'(x)^2+\varsigma_2^2\overline{F}_0'(x)^4)+(3\varsigma_1-\varsigma_2)\overline{F}_0'(x)^2\overline{F}_0''(x)+\varsigma_1\varsigma_2\overline{F}_0'(x)^4\overline{F}_0''(x)+\overline{F}_1''(x)=0,\quad \overline{F}_0(0)=0,\quad \overline{F}_0'(1)=0, \tag{52}$$

$$\begin{aligned}\overline{F}_1(x;\alpha)=&\frac{1}{2}g_r(1.82648-0.33059\alpha)(0.95+0.02\gamma)^{2.5}x\times\left(-2+x-4.\times10^{-6}(-1.+\alpha)^2\zeta_2+2.\times10^{-6}(-1.+\alpha)^2x\zeta_2\right.\\ &\left.-2.\times10^{-12}(-1.+\alpha)^4\zeta_2^2+1.\times10^{-12}\zeta_2^2(-1.+\alpha)^4x\right)\end{aligned} \tag{53}$$

The kth-order fuzzy solution up-to 4th order deformation equation is:

$$\tilde{F}(x;\alpha)=[\underline{F}(x;\alpha),\ \overline{F}(x;a)]=[\underline{F_0}(x;\alpha),\ \overline{F}_0(x;a)]+[\underline{F_1}(x;\alpha),\ \overline{F}_1(x;a)]+[\underline{F_2}(x;\alpha),\ \overline{F}_2(x;a)]+\ldots \tag{54}$$

5.5. Formulation of Oldroyd 6-Constant Nanofluid in Drainage Scenario

Now let's examine the scenario where fluid falls onto an unmovable, stationary belt. Gravity pulls the flow downwards, causing Eq. (42) to transform into:

$$\frac{d^2F}{dx^2}+(3\varsigma_1-\varsigma_2)\left(\frac{dF}{dx}\right)^2\frac{d^2F}{dx^2}+\varsigma_1\varsigma_2\left(\frac{dF}{dx}\right)^4\frac{d^2F}{dx^2}+\frac{D_1}{D_2}g_r\left(1+\varsigma_2\left(\frac{dF}{dx}\right)^2\right)^2=0, \tag{55}$$

subject to:

$$\begin{aligned} &F(x)=0 \quad \text{at} \quad x=0. \\ &\frac{dF}{dx}=0 \quad \text{at} \quad x=1. \end{aligned} \tag{56}$$

By applying fundamental definitions of fractional calculus, Eq. (55) is transformed into the subsequent fractional differential equation:

$$\frac{d^{\beta}F}{dx^{\beta}}+(3\varsigma_1-\varsigma_2)\left(\frac{dF}{dx}\right)^2\frac{d^{\beta}F}{dx^{\beta}}+\varsigma_1\varsigma_2\left(\frac{dF}{dx}\right)^4\frac{d^{\beta}F}{dx^{\beta}}+\frac{D_1}{D_2}g_r\left(1+\varsigma_2\left(\frac{dF}{dx}\right)^2\right)^2=0, \tag{57}$$

with boundary conditions:

$$\begin{aligned} &F(x)=0 \quad \text{at} \quad x=0, \\ &\frac{dF}{dx}=0 \quad \text{at} \quad x=1, \qquad 1<\beta\le 2. \end{aligned} \tag{58}$$

5.6. Fuzzification of Fractional Oldroyd 6-Constant Nanofluid in Drainage Case

By utilizing the fuzzy numbers, we can modify Eq. (57) to incorporate the degree of fuzziness:

$$\left[\frac{d^{\beta}(\underline{F})}{dx^{\beta}},\frac{d^{\beta}(\overline{F})}{dx^{\beta}}\right]+[3\zeta_1-\zeta_2]\left[\left(\frac{d(\underline{F})}{dx}\right)^2,\left(\frac{d(\overline{F})}{dx}\right)^2\right]\left[\frac{d^{\beta}(\underline{F})}{dx^{\beta}},\frac{d^{\beta}(\overline{F})}{dx^{\beta}}\right]+\zeta_1\zeta_2\left[\left(\frac{d(\underline{F})}{dx}\right)^4,\left(\frac{d(\overline{F})}{dx}\right)^4\right]\left[\frac{d^{\beta}(\underline{F})}{dx^{\beta}},\frac{d^{\beta}(\overline{F})}{dx^{\beta}}\right]+\frac{D_1}{D_2}g_r\left(1+\zeta_2\left[\left(\frac{d(\underline{F})}{dx}\right)^2,\left(\frac{d(\overline{F})}{dx}\right)^2\right]\right)^2=0, \tag{59}$$

where, $D_1=(1-\eta)+\eta(\rho_s/\rho_f)$, and $D_2=1/(1-\eta)^{2.5}$ with fuzzy condition as Eq. (45) along with the TFN's $\tilde{A}=(-0.02,0,0.02)$, $\tilde{B}=(-0.001,0,0.001)$, and $\eta=(0.001,0.03,0.05)$ have $\alpha-$cut expressed as $[0.02\alpha-0.02,0.02-0.02\alpha]$,$[0.001(\alpha-1),0.001(1-\alpha)]$, and $[0.001+0.029\alpha,0.05-0.02\alpha]$, respectively.

5.7. Solution of Fuzzy-Fractional Model in Draining Case

We can expend $\underline{F}$ and $\overline{F}$ in Taylor series form as:

$$\underline{F}=\sum_{i=0}^{\infty}p^i\underline{F}_i, \tag{60}$$

$$\overline{F}=\sum_{i=0}^{\infty}p^i\overline{F}_i, \tag{61}$$

where, $\underline{F}_i,\overline{F}_i$ correspond to the ith-order lower and upper deformation velocity profiles. Putting fractional order $\beta=2$ along with Eqs. (60) and (61) in Eq. (59) and compare the coefficients of like powers of p gives the following deformation equations:

0th-order fuzzy problem and solution:

$$\begin{aligned} &\underline{F}_0''(x)=0,\ \underline{F}_0(0)=0.02\alpha-0.02,\ \underline{F}_0'(1)=0.001\alpha-0.001, \\ &\underline{F}_0(x;\alpha)=-0.02+0.02\alpha+(-0.001+0.001\alpha)x. \end{aligned} \tag{62}$$

$$\begin{aligned} &\overline{F}_0''(x)=0,\ \overline{F}_0(0)=0.02-0.02\alpha,\ \overline{F}_0'(1)=0.001-0.001\alpha, \\ &\overline{F}_0(x;\alpha)=0.02-0.02\alpha+(0.001-0.001\alpha)x. \end{aligned} \tag{63}$$

1st-order fuzzy problem and solution:

$$-\frac{D_1}{D_2}g_r\left(1+2\varsigma_2\underline{F_0'}(x)^2+\varsigma_2^2\underline{F_0'}(x)^4\right)+(3\varsigma_1-\varsigma_2)\underline{F_0'}(x)^2\underline{F_0''}(x)+\varsigma_1\varsigma_2\underline{F_0'}(x)^4\underline{F_0''}(x)+\underline{F_1''}(x)=0,\quad \underline{F}_0(0)=0,\quad \underline{F_0'}(1)=0, \tag{64}$$

$$\begin{aligned} \underline{F}_1(x;\alpha)=\frac{1}{2}\ &g_r(0.999-0.029\alpha)^{2.5}(1.01653+0.479356\alpha)x\times\Big(2-x+4(0.001-0.001\alpha)^2\zeta_2-2\times10^{-6}(1-1.\alpha)^2x\zeta_2 \\ &+2(0.001-0.001\alpha)\zeta_2^2-1\times10^{-12}\zeta_2^2(1-1.\alpha)^4x\Big). \end{aligned} \tag{65}$$

$$-\frac{D_1}{D_2}g_r(1+2\varsigma_2\overline{F_0'}(x)^2+\varsigma_2^2\overline{F_0'}(x)^4)+(3\varsigma_1-\varsigma_2)\overline{F_0'}(x)^2\overline{F_0''}(x)+\varsigma_1\varsigma_2\overline{F_0'}(x)^4\overline{F_0''}(x)+\overline{F_1''}(x)=0,\ \overline{F_0}(0)=0,\ \overline{F_0'}(1)=0, \tag{66}$$

$$\begin{aligned} \overline{F}_1(x;\alpha)\ =\frac{1}{2}\ &g_r(1.82648-0.33059\alpha)(0.95+0.02r)^{2.5}x\times\Big(2-x+4(0.001-0.001\alpha)^2\zeta_2-2\times10^{-6}(1-1.\alpha)^2x\zeta_2 \\ &+2(0.001-0.001\alpha)^4\zeta_2^2-1\times10^{-12}\zeta_2^2(1-1.\alpha)^4x\Big). \end{aligned} \tag{67}$$

The kth-order fuzzy solution up-to 4th order deformation equation is:

$$\tilde{F}(x;\alpha)=[\underline{F}(x;\alpha),\ \overline{F}(x;a)\,]=[\underline{F_0}(x;\alpha),\ \overline{F}_0(x;a)\,]+[\underline{F_1}(x;\alpha),\ \overline{F}_1(x;a)\,]+[\underline{F_2}(x;\alpha),\ \overline{F}_2(x;a)\,]+\ldots \tag{68}$$

Table 1. Thermo-physical properties of base fluid and nano-particles.

Base Fluid/Nanoparticles	$\rho(kg/m^3)$	$C_p(J/kg.K)$
Gold	19300	129
Silver	10500	235
Alumina	3970	765
Water	997	4179

Table 2. Fuzzy solution and error analysis for the impact of ζ_1 when $\alpha=0.8, g_r=0.1, \beta=2, \zeta_2=0.1$.

$\alpha=0.8$	$\zeta_1=0.3$				
	x	Sol.	Abs. Residual Error		
			HPM	RK-Fehlberg	C-Nicklson
$\underline{F}$	0.0	0.84	2.64×10^{-4}	2.41×10^{-12}	4.15×10^{-6}
	0.2	0.816325	1.09×10^{-4}	9.08×10^{-14}	4.29×10^{-6}
	0.4	0.797881	3.45×10^{-6}	3.13×10^{-15}	4.41×10^{-6}
	0.6	0.784684	6.88×10^{-7}	2.85×10^{-14}	4.49×10^{-6}
	0.8	0.776746	4.41×10^{-8}	9.04×10^{-13}	4.58×10^{-6}
	1.0	0.774073	2.78×10^{-17}	2.49×10^{-11}	4.57×10^{-6}
$\overline{F}$	0.0	1.02	3.93×10^{-4}	7.59×10^{-12}	5.24×10^{-6}
	0.2	0.99434	1.61×10^{-4}	1.75×10^{-14}	5.46×10^{-6}
	0.4	0.974364	5.09×10^{-6}	4.71×10^{-15}	5.64×10^{-6}
	0.6	0.960093	1.00×10^{-6}	3.72×10^{-14}	5.77×10^{-6}
	0.8	0.951541	6.12×10^{-8}	1.96×10^{-14}	5.85×10^{-6}
	1.0	0.948716	5.55×10^{-17}	1.38×10^{-11}	5.89×10^{-6}

$\alpha=0.8$	$\zeta_1=0.3$				
	x	Sol.	Abs. Residual Error		
			HPM	RK-Fehlberg	C-Nicklson
$\underline{F}$	0.0	0.84	2.64×10^{-4}	1.91×10^{-12}	7.62×10^{-6}
	0.2	0.816392	1.09×10^{-4}	2.56×10^{-13}	8.13×10^{-6}
	0.4	0.797981	3.45×10^{-6}	1.28×10^{-15}	8.56×10^{-6}
	0.6	0.784796	6.88×10^{-7}	9.99×10^{-14}	8.87×10^{-6}
	0.8	0.776861	4.41×10^{-8}	2.53×10^{-12}	9.06×10^{-6}
	1.0	0.774187	2.78×10^{-17}	5.30×10^{-11}	9.13×10^{-6}
$\overline{F}$	0.0	1.02	1.52×10^{-3}	2.28×10^{-11}	9.49×10^{-6}
	0.2	0.994426	6.23×10^{-4}	5.60×10^{-13}	1.03×10^{-4}
	0.4	0.974491	1.97×10^{-4}	2.11×10^{-14}	1.08×10^{-4}
	0.6	0.960236	3.88×10^{-6}	2.17×10^{-13}	1.14×10^{-4}
	0.8	0.951687	2.39×10^{-7}	5.23×10^{-12}	1.16×10^{-4}
	1.0	0.948862	5.55×10^{-17}	1.38×10^{-10}	1.18×10^{-4}

Table 3. Fuzzy solution and error analysis for the impact of ζ_2 when $\alpha=0.3, g_r=0.05, \beta=2, \zeta_1=0.1$.

$\alpha=0.3$	$\zeta_2=0.5$				
	x	Sol.	Abs. Residual Error		
			HPM	RK-Fehlberg	C-Nicklson
$\underline{F}$	0.0	0.44	2.86×10^{-7}	1.66×10^{-12}	7.39×10^{-7}
	0.2	0.429657	1.17×10^{-7}	1.23×10^{-14}	7.34×10^{-7}
	0.4	0.421585	3.69×10^{-8}	7.99×10^{-15}	7.13×10^{-7}
	0.6	0.415781	7.33×10^{-9}	8.58×10^{-15}	7.28×10^{-7}
	0.8	0.412243	4.66×10^{-10}	1.61×10^{-14}	7.27×10^{-7}
	1.0	0.410971	6.94×10^{-18}	1.59×10^{-12}	7.26×10^{-7}
$\overline{F}$	0.0	1.07	1.34×10^{-6}	9.10×10^{-13}	1.90×10^{-6}
	0.2	1.05622	5.44×10^{-7}	5.15×10^{-15}	1.88×10^{-6}
	0.4	1.04554	1.71×10^{-7}	2.40×10^{-15}	1.86×10^{-6}
	0.6	1.03796	3.35×10^{-8}	2.18×10^{-15}	1.85×10^{-6}
	0.8	1.03347	2.07×10^{-9}	1.71×10^{-14}	1.84×10^{-6}
	1.0	1.03207	0	1.05×10^{-13}	1.84×10^{-13}

$\alpha=0.3$	$\zeta_2=1.0$				
	x	Sol.	Abs. Residual Error		
			HPM	RK-Fehlberg	C-Nicklson
$\underline{F}$	0.0	0.44	2.37×10^{-6}	6.61×10^{-13}	1.71×10^{-6}
	0.2	0.429643	9.69×10^{-7}	7.74×10^{-15}	1.68×10^{-6}
	0.4	0.421564	3.07×10^{-7}	1.28×10^{-15}	1.66×10^{-6}
	0.6	0.415758	6.91×10^{-8}	9.53×10^{-15}	1.65×10^{-6}
	0.8	0.412219	3.89×10^{-9}	1.73×10^{-14}	1.64×10^{-6}
	1.0	0.410947	2.08×10^{-17}	7.55×10^{-13}	1.63×10^{-6}
$\overline{F}$	0.0	1.07	1.11×10^{-4}	7.74×10^{-12}	4.49×10^{-6}
	0.2	1.05619	4.49×10^{-6}	3.42×10^{-14}	4.36×10^{-6}
	0.4	1.0455	1.41×10^{-6}	1.89×10^{-14}	4.26×10^{-6}
	0.6	1.03791	2.76×10^{-7}	4.43×10^{-14}	4.19×10^{-6}
	0.8	1.03342	1.68×10^{-8}	1.70×10^{-14}	4.15×10^{-6}
	1.0	1.03201	2.78×10^{-17}	8.96×10^{-12}	4.13×10^{-6}

Table 4. Fuzzy solution and error analysis for the impact of g_r when $\alpha=0.9, \zeta_2=0.05, \beta=2, \zeta_1=0.1$.

$\alpha=0.9$	$g_r=0.1$				
	x	Sol.	Abs. Residual Error		
			HPM	RK-Fehlberg	C-Nicklson
$\underline{F}$	0.0	0.92	7.39×10^{-6}	1.66×10^{-13}	2.33×10^{-6}
	0.2	0.895683	3.04×10^{-6}	2.58×10^{-15}	2.38×10^{-6}
	0.4	0.876755	9.66×10^{-7}	9.27×10^{-15}	2.41×10^{-6}
	0.6	0.863223	1.92×10^{-7}	5.55×10^{-15}	2.45×10^{-6}
	0.8	0.855094	1.23×10^{-8}	1.33×10^{-14}	2.46×10^{-6}
	1.0	0.85237	2.76×10^{-17}	1.72×10^{-13}	2.47×10^{-6}
$\overline{F}$	0.0	1.01	8.97×10^{-6}	3.29×10^{-12}	2.63×10^{-6}
	0.2	0.984689	3.67×10^{-6}	1.44×10^{-14}	2.69×10^{-6}
	0.4	0.964995	1.61×10^{-6}	1.47×10^{-14}	2.73×10^{-6}
	0.6	0.950927	2.28×10^{-7}	1.69×10^{-14}	2.77×10^{-6}
	0.8	0.942491	1.40×10^{-8}	8.07×10^{-15}	2.79×10^{-6}
	1.0	0.939692	2.78×10^{-17}	1.91×10^{-12}	2.80×10^{-6}

$\alpha=0.9$	$g_r=0.3$				
	x	Sol.	Abs. Residual Error		
			HPM	RK-Fehlberg	C-Nicklson
$\underline{F}$	0.0	0.92	2.32×10^{-3}	1.97×10^{-9}	3.86×10^{-4}
	0.2	0.871605	9.59×10^{-6}	1.85×10^{-11}	4.73×10^{-4}
	0.4	0.833871	3.05×10^{-4}	1.08×10^{-12}	5.51×10^{-4}
	0.6	0.806866	6.07×10^{-6}	2.08×10^{-12}	6.13×10^{-4}
	0.8	0.790636	3.84×10^{-7}	3.65×10^{-11}	6.53×10^{-4}
	1.0	0.785209	5.55×10^{-17}	1.41×10^{-9}	6.67×10^{-4}
$\overline{F}$	0.0	1.01	1.11×10^{-4}	7.74×10^{-12}	4.49×10^{-6}
	0.2	0.959605	4.49×10^{-6}	3.42×10^{-14}	4.36×10^{-6}
	0.4	0.920314	1.41×10^{-6}	1.89×10^{-14}	4.26×10^{-6}
	0.6	0.892201	2.76×10^{-7}	4.43×10^{-14}	4.19×10^{-6}
	0.8	0.87532	1.68×10^{-8}	1.70×10^{-14}	4.15×10^{-6}
	1.0	0.869702	2.78×10^{-17}	8.96×10^{-12}	4.13×10^{-6}

Table 5. Fuzzy solution and error analysis for the impact of ζ_1 when $\alpha=0.6, g_r=0.1, \beta=2, \zeta_2=0.2$.

$\alpha=0.6$	$\zeta_1=0.1$				
	x	Sol.	Abs. Residual Error		
			HPM	RK-Fehlberg	C-Nicklson
$\underline{F}$	0.0	-0.008	2.89×10^{-6}	2.80×10^{-13}	1.95×10^{-6}
	0.2	0.01435	1.18×10^{-6}	3.05×10^{-16}	1.94×10^{-6}
	0.4	0.03172	3.76×10^{-7}	3.33×10^{-16}	1.94×10^{-6}
	0.6	0.04409	7.44×10^{-8}	1.59×10^{-15}	1.93×10^{-6}
	0.8	0.05148	4.68×10^{-9}	1.08×10^{-14}	1.93×10^{-6}
	1.0	0.05389	1.39×10^{-17}	1.54×10^{-14}	1.92×10^{-6}
$\overline{F}$	0.0	0.008	6.79×10^{-6}	1.76×10^{-13}	3.28×10^{-6}
	0.2	0.03472	2.78×10^{-7}	1.05×10^{-15}	3.26×10^{-6}
	0.4	0.05552	8.80×10^{-7}	1.75×10^{-15}	3.25×10^{-6}
	0.6	0.07038	1.73×10^{-8}	9.44×10^{-16}	3.24×10^{-6}
	0.8	0.07934	1.08×10^{-8}	4.16×10^{-16}	3.23×10^{-6}
	1.0	0.08237	0	1.54×10^{-14}	3.23×10^{-14}

$\alpha=0.6$	$\zeta_1=0.5$				
	x	Sol.	Abs. Residual Error		
			HPM	RK-Fehlberg	C-Nicklson
$\underline{F}$	0.0	-0.008	4.35×10^{-4}	1.59×10^{-12}	5.05×10^{-6}
	0.2	0.01424	1.78×10^{-4}	1.50×10^{-14}	5.31×10^{-6}
	0.4	0.03155	5.57×10^{-6}	7.63×10^{-16}	5.51×10^{-6}
	0.6	0.04391	1.08×10^{-6}	1.96×10^{-15}	5.66×10^{-6}
	0.8	0.05129	6.32×10^{-8}	1.22×10^{-14}	5.76×10^{-6}
	1.0	0.053701	1.39×10^{-17}	1.09×10^{-13}	5.79×10^{-6}
$\overline{F}$	0.0	0.008	1.07×10^{-4}	8.49×10^{-12}	7.97×10^{-6}
	0.2	0.03453	4.42×10^{-4}	8.36×10^{-14}	8.55×10^{-6}
	0.4	0.05523	1.41×10^{-4}	5.83×10^{-16}	9.03×10^{-6}
	0.6	0.07007	2.85×10^{-6}	9.08×10^{-15}	9.38×10^{-6}
	0.8	0.07901	1.87×10^{-7}	6.87×10^{-14}	9.60×10^{-6}
	1.0	0.08205	0	8.73×10^{-12}	9.68×10^{-6}

6. Results and Discussion

The focus of this article is to study fuzzy-fractional thin film flow of Oldroyd 6-constant nanofluid. Fuzzification is done through volume fraction of nanoparticles and boundary conditions. The primary objective of this investigation is to evaluate the impact of different parameters namely gravitational parameter g_r and material parameters ζ_1 and ζ_2 along with fuzzy volume fraction α on the velocity profile. The problem is modeled and analyzed through numerical and semi-numerical techniques and findings are presented in both tabular and graphical formats. Table 1 show the values of thermo-physical properties of base fluid and nano-particles which helps to developed the graphical approach, Tables 2 to 4 illustrate the fuzzy solutions and corresponding errors in lifting and drainage cases respectively at different values of ζ_1, ζ_2 and g_r keeping fuzzy parameter α between 0 and 1.

Table 6. Fuzzy solution and error analysis for the impact of ζ_2 when $\alpha = 0.3, g_r = 0.05, \beta = 2, \zeta_1 = 0.1$.

			$\zeta_2 = 0.5$		
$\alpha = 0.3$	x	Sol.	Abs. Residual Error		
			HPM	RK-Fehlberg	C-Nicklson
$\underline{F}$	0.0	-0.014	2.82×10^{-7}	2.74×10^{-13}	7.39×10^{-7}
	0.2	-0.00393	1.15×10^{-7}	2.48×10^{-15}	7.34×10^{-7}
	0.4	0.003853	361×10^{-8}	4.93×10^{-16}	7.30×10^{-7}
	0.6	0.009377	7.08×10^{-9}	2.78×10^{-17}	7.28×10^{-7}
	0.8	0.012635	4.35×10^{-10}	2.21×10^{-15}	7.27×10^{-7}
	1.0	0.013627	6.94×10^{-18}	2.71×10^{-13}	7.26×10^{-7}
$\overline{F}$	0.0	0.014	1.35×10^{-6}	1.52×10^{-12}	1.90×10^{-6}
	0.2	0.02805	5.51×10^{-7}	9.94×10^{-15}	1.87×10^{-6}
	0.4	0.03902	1.74×10^{-7}	4.16×10^{-17}	1.86×10^{-6}
	0.6	0.046880	3.43×10^{-8}	3.75×10^{-16}	1.85×10^{-6}
	0.8	0.051652	2.17×10^{-9}	7.13×10^{-15}	1.84×10^{-6}
	1.0	0.053336	0	8.96×10^{-13}	1.83×10^{-14}
			$\zeta_2 = 1.0$		
$\alpha = 0.3$	x	Sol.	Abs. Residual Error		
			HPM	RK-Fehlberg	C-Nicklson
$\underline{F}$	0.0	-0.014	2.32×10^{-6}	1.87×10^{-12}	1.70×10^{-6}
	0.2	-0.00392	9.45×10^{-7}	1.19×10^{-14}	1.68×10^{-6}
	0.4	0.003872	2.96×10^{-8}	0	1.65×10^{-6}
	0.6	0.009398	5.79×10^{-9}	3.19×10^{-16}	1.64×10^{-6}
	0.8	0.012656	3.52×10^{-9}	9.53×10^{-15}	1.64×10^{-6}
	1.0	0.013649	2.08×10^{-17}	1.63×10^{-12}	1.63×10^{-6}
$\overline{F}$	0.0	0.014	1.13×10^{-4}	9.73×10^{-12}	4.49×10^{-6}
	0.2	0.02809	4.58×10^{-6}	5.49×10^{-14}	4.36×10^{-6}
	0.4	0.03907	1.44×10^{-6}	7.91×10^{-15}	4.26×10^{-6}
	0.6	0.04694	2.86×10^{-7}	5.41×10^{-15}	4.19×10^{-6}
	0.8	0.05171	1.81×10^{-8}	2.00×10^{-14}	4.15×10^{-6}
	1.0	0.05339	2.78×10^{-17}	5.69×10^{-12}	4.13×10^{-6}

Table 7. Fuzzy solution and error analysis for the impact of g_r when $\alpha = 0.2, \zeta_2 = 0.2, \beta = 2, \zeta_1 = 0.1$.

			$g_r = 0.1$		
$\alpha = 0.9$	x	Sol.	Abs. Residual Error		
			HPM	RK-Fehlberg	C-Nicklson
$\underline{F}$	0.0	-0.002	7.28×10^{-6}	2.13×10^{-13}	2.33×10^{-6}
	0.2	0.02227	2.98×10^{-6}	2.22×10^{-15}	2.38×10^{-6}
	0.4	0.04117	9.42×10^{-7}	1.94×10^{-15}	2.42×10^{-6}
	0.6	0.05465	1.85×10^{-7}	2.28×10^{-15}	2.44×10^{-6}
	0.8	0.06274	1.14×10^{-8}	2.01×10^{-14}	2.46×10^{-6}
	1.0	0.06543	9.10×10^{-17}	6.31×10^{-13}	2.47×10^{-6}
$\overline{F}$	0.0	0.002	9.10×10^{-6}	1.10×10^{-12}	2.63×10^{-6}
	0.2	0.02735	3.74×10^{-6}	5.13×10^{-15}	2.69×10^{-6}
	0.4	0.04708	1.19×10^{-6}	1.25×10^{-17}	2.73×10^{-6}
	0.6	0.06119	2.37×10^{-7}	1.30×10^{-16}	2.77×10^{-6}
	0.8	0.06966	1.51×10^{-8}	1.93×10^{-14}	2.79×10^{-6}
	1.0	0.07251	2.78×10^{-17}	7.00×10^{-17}	2.80×10^{-6}
			$g_r = 0.3$		
$\alpha = 0.9$	x	Sol.	Abs. Residual Error		
			HPM	RK-Fehlberg	C-Nicklson
$\underline{F}$	0.0	-0.002	1.71×10^{-2}	2.35×10^{-9}	3.87×10^{-4}
	0.2	0.07001	7.10×10^{-3}	2.25×10^{-11}	4.73×10^{-4}
	0.4	0.012629	2.27×10^{-3}	1.07×10^{-12}	5.51×10^{-4}
	0.6	0.016666	4.52×10^{-4}	4.14×10^{-12}	6.13×10^{-4}
	0.8	0.019094	2.83×10^{-6}	9.06×10^{-11}	5.53×10^{-4}
	1.0	0.019902	0	3.93×10^{-10}	6.67×10^{-4}
$\overline{F}$	0.0	0.002	2.11×10^{-2}	3.38×10^{-9}	4.16×10^{-4}
	0.2	0.07703	8.79×10^{-3}	3.24×10^{-11}	5.19×10^{-4}
	0.4	0.13572	2.82×10^{-3}	1.49×10^{-12}	6.14×10^{-4}
	0.6	0.17783	5.64×10^{-4}	6.27×10^{-12}	6.89×10^{-4}
	0.8	0.20318	3.57×10^{-6}	1.27×10^{-10}	7.38×10^{-4}
	1.0	0.21166	5.55×10^{-17}	2.67×10^{-10}	7.56×10^{-4}

Table 8. Fuzzy solution and error analysis for the impact of ζ_2 when $g_r = 0.11, \beta = 2, \zeta_1 = 0.4$.

			$\zeta_2 = 0.5$		
x = 0.7	α	Sol.	Abs. Residual Error		
			HPM	RK-Fehlberg	C-Nicklson
$\underline{F}$	0.0	0.148514	1.29×10^{-7}	1.66×10^{-13}	1.36×10^{-6}
	0.2	0.304661	1.93×10^{-7}	2.58×10^{-15}	1.74×10^{-6}
	0.4	0.460938	2.77×10^{-7}	9.27×10^{-15}	2.13×10^{-6}
	0.6	0.617343	3.85×10^{-7}	5.55×10^{-15}	2.56×10^{-6}
	0.8	0.773874	5.18×10^{-7}	1.33×10^{-14}	3.03×10^{-6}
	1.0	0.93053	6.97×10^{-7}	1.72×10^{-13}	3.53×10^{-6}
$\overline{F}$	0.0	1.02015	1.51×10^{-6}	3.29×10^{-12}	5.49×10^{-6}
	0.2	1.00211	1.31×10^{-6}	1.44×10^{-14}	5.08×10^{-6}
	0.4	0.98413	1.13×10^{-6}	1.47×10^{-14}	4.67×10^{-6}
	0.6	0.966206	9.60×10^{-7}	1.69×10^{-14}	4.28×10^{-6}
	0.8	0.948339	8.12×10^{-7}	8.07×10^{-15}	3.89×10^{-6}
	1.0	0.93053	6.79×10^{-7}	1.91×10^{-12}	3.53×10^{-6}
			$\zeta_2 = 1.0$		
x = 0.7	α	Sol.	Abs. Residual Error		
			HPM	RK-Fehlberg	C-Nicklson
$\underline{F}$	0.0	0.148334	1.76×10^{-7}	4.62×10^{-14}	8.38×10^{-6}
	0.2	0.304437	2.56×10^{-7}	1.91×10^{-13}	1.05×10^{-4}
	0.4	0.460665	3.61×10^{-7}	2.61×10^{-13}	1.29×10^{-4}
	0.6	0.617016	4.91×10^{-7}	1.79×10^{-13}	1.56×10^{-4}
	0.8	0.773489	6.52×10^{-7}	1.03×10^{-13}	1.85×10^{-4}
	1.0	0.930083	8.42×10^{-7}	6.75×10^{-13}	2.16×10^{-4}
$\overline{F}$	0.0	1.01946	1.77×10^{-7}	1.17×10^{-12}	3.38×10^{-4}
	0.2	0.00148	1.55×10^{-6}	8.44×10^{-13}	3.12×10^{-4}
	0.4	0.983554	1.35×10^{-6}	7.15×10^{-13}	2.86×10^{-4}
	0.6	0.965668	1.16×10^{-6}	1.04×10^{-12}	2.62×10^{-4}
	0.8	0.947874	9.93×10^{-7}	7.46×10^{-12}	2.38×10^{-4}
	1.0	0.930083	8.42×10^{-7}	6.75×10^{-13}	2.16×10^{-4}

Table 9. Fuzzy solution and error analysis for the impact of g_r when $x = 1, \zeta_2 = 0.2, \beta = 2, \zeta_1 = 0.1$.

			$g_r = 0.2$		
x = 1.0	α	Sol.	Abs. Residual Error		
			HPM	RK-Fehlberg	C-Nicklson
$\underline{F}$	0.0	0.0973866	1.47×10^{-17}	8.99×10^{-12}	8.34×10^{-6}
	0.2	0.249573	0	2.54×10^{-12}	1.05×10^{-4}
	0.4	0.402015	2.78×10^{-17}	2.61×10^{-11}	2.42×10^{-4}
	0.6	0.554709	2.78×10^{-17}	5.56×10^{-14}	1.54×10^{-4}
	0.8	0.707651	5.55×10^{-17}	7.95×10^{-13}	1.83×10^{-4}
	1.0	0.860839	0	5.54×10^{-12}	2.13×10^{-4}
$\overline{F}$	0.0	1.02015	5.55×10^{-17}	4.26×10^{-12}	3.31×10^{-4}
	0.2	1.00211	0	1.65×10^{-12}	3.07×10^{-4}
	0.4	0.98413	5.55×10^{-17}	3.24×10^{-11}	2.91×10^{-4}
	0.6	0.966206	0	7.56×10^{-13}	2.58×10^{-4}
	0.8	0.948339	0	4.53×10^{-12}	2.35×10^{-4}
	1.0	0.93053	0	5.54×10^{-12}	2.13×10^{-4}
			$g_r = 0.5$		
x = 1.0	α	Sol.	Abs. Residual Error		
			HPM	RK-Fehlberg	C-Nicklson
$\underline{F}$	0.0	0.148334	2.22×10^{-16}	4.12×10^{-10}	1.30×10^{-3}
	0.2	0.304437	0	5.57×10^{-10}	1.64×10^{-3}
	0.4	0.460665	2.22×10^{-16}	2.29×10^{-9}	2.01×10^{-3}
	0.6	0.617016	0	3.04×10^{-9}	3.04×10^{-3}
	0.8	0.773489	1.11×10^{-16}	6.97×10^{-9}	5.06×10^{-3}
	1.0	0.930083	0	1.18×10^{-8}	3.33×10^{-3}
$\overline{F}$	0.0	1.01946	2.22×10^{-16}	4.23×10^{-8}	5.19×10^{-3}
	0.2	0.00148	1.11×10^{-16}	3.17×10^{-8}	4.49×10^{-3}
	0.4	0.983554	1.11×10^{-17}	3.28×10^{-8}	4.41×10^{-3}
	0.6	0.965668	0	1.79×10^{-8}	4.04×10^{-3}
	0.8	0.947874	0	8.58×10^{-9}	3.68×10^{-3}
	1.0	0.930083	0	1.18×10^{-8}	3.33×10^{-3}

Table 10. Fuzzy solution and error analysis for the impact of ζ_2 when $g_r = 0.11, \beta = 2, \zeta_1 = 0.4$.

$x = 0.7$	$\zeta_2 = 0.5$				
	α	Sol.	Abs. Residual Error		
			HPM	RK-Fehlberg	C-Nicklson
$\underline{F}$	0.0	0.030084	1.56×10^{-7}	6.25×10^{-16}	1.39×10^{-6}
	0.2	0.0382168	2.22×10^{-7}	5.41×10^{-16}	1.74×10^{-6}
	0.4	0.0462201	3.06×10^{-7}	1.64×10^{-15}	2.13×10^{-6}
	0.6	0.0540956	4.09×10^{-7}	1.33×10^{-15}	2.56×10^{-6}
	0.8	0.061845	5.34×10^{-7}	9.71×10^{-16}	3.03×10^{-6}
	1.0	0.06947	6.79×10^{-7}	5.83×10^{-15}	3.53×10^{-6}
$\overline{F}$	0.0	0.101258	1.13×10^{-6}	1.83×10^{-16}	5.49×10^{-6}
	0.2	0.0950139	1.18×10^{-6}	8.88×10^{-15}	5.08×10^{-6}
	0.4	0.0887135	1.04×10^{-6}	2.55×10^{-17}	4.67×10^{-6}
	0.6	0.0823564	9.12×10^{-7}	3.52×10^{-15}	4.28×10^{-6}
	0.8	0.0759421	7.90×10^{-7}	8.05×10^{-15}	3.89×10^{-6}
	1.0	0.06947	6.79×10^{-7}	5.83×10^{-15}	3.53×10^{-6}
$x = 0.7$	$\zeta_2 = 1.0$				
	x	Sol.	Abs. Residual Error		
			HPM	RK-Fehlberg	C-Nicklson
$\underline{F}$	0.0	0.0302515	1.78×10^{-7}	3.99×10^{-14}	8.38×10^{-6}
	0.2	0.0384293	2.59×10^{-7}	1.37×10^{-15}	1.05×10^{-4}
	0.4	0.0464832	3.63×10^{-7}	1.48×10^{-15}	1.29×10^{-4}
	0.6	0.0544147	4.93×10^{-7}	1.26×10^{-14}	1.56×10^{-4}
	0.8	0.0622256	6.52×10^{-7}	5.99×10^{-14}	1.85×10^{-4}
	1.0	0.0699172	8.42×10^{-7}	7.19×10^{-14}	2.16×10^{-4}
$\overline{F}$	0.0	0.101974	1.75×10^{-6}	3.43×10^{-13}	3.38×10^{-4}
	0.2	0.0956722	1.53×10^{-6}	5.35×10^{-13}	3.12×10^{-4}
	0.4	0.0893158	1.33×10^{-6}	3.59×10^{-14}	2.86×10^{-4}
	0.6	0.0829048	1.16×10^{-6}	2.88×10^{-14}	2.62×10^{-4}
	0.8	0.0764387	9.91×10^{-7}	3.42×10^{-13}	2.38×10^{-4}
	1.0	0.0699172	8.42×10^{-7}	7.19×10^{-14}	2.16×10^{-4}

Table 11. Fuzzy solution and error analysis for the impact of g_r when $\zeta_2 = 0.2, \beta = 2, \zeta_1 = 0.1$.

$x = 1.0$	$g_r = 0.2$				
	α	Sol.	Abs. Residual Error		
			HPM	RK-Fehlberg	C-Nicklson
$\underline{F}$	0.0	0.0806051	2.78×10^{-17}	1.49×10^{-12}	8.34×10^{-6}
	0.2	0.0928188	0	8.93×10^{-13}	1.05×10^{-4}
	0.4	0.104778	2.78×10^{-17}	1.28×10^{-4}	2.42×10^{-4}
	0.6	0.116486	2.78×10^{-17}	4.67×10^{-11}	1.54×10^{-4}
	0.8	0.127946	5.55×10^{-17}	7.09×10^{-11}	1.83×10^{-4}
	1.0	0.139161	0	3.14×10^{-11}	2.13×10^{-4}
$\overline{F}$	0.0	0.182522	5.55×10^{-17}	2.24×10^{-10}	3.31×10^{-4}
	0.2	0.174074	0	1.73×10^{-10}	3.07×10^{-4}
	0.4	0.165514	5.55×10^{-17}	2.82×10^{-4}	2.91×10^{-4}
	0.6	0.156843	0	1.81×10^{-11}	2.58×10^{-4}
	0.8	0.148059	0	6.73×10^{-11}	2.35×10^{-4}
	1.0	0.139161	0	3.14×10^{-11}	2.13×10^{-4}
$\alpha = 0.9$	$g_r = 0.5$				
	x	Sol.	Abs. Residual Error		
			HPM	RK-Fehlberg	C-Nicklson
$\underline{F}$	0.0	0.235893	2.22×10^{-16}	3.74×10^{-10}	1.30×10^{-3}
	0.2	0.260898	0	1.46×10^{-10}	1.64×10^{-3}
	0.4	0.28537	2.22×10^{-16}	1.39×10^{-9}	2.01×10^{-3}
	0.6	0.309316	0	4.38×10^{-9}	2.41×10^{-3}
	0.8	0.332743	1.11×10^{-16}	6.97×10^{-9}	2.86×10^{-3}
	1.0	0.355657	0	1.31×10^{-8}	3.33×10^{-3}
$\overline{F}$	0.0	0.437328	2.22×10^{-16}	5.32×10^{-8}	5.19×10^{-3}
	0.2	0.421471	1.11×10^{-16}	4.08×10^{-8}	4.79×10^{-3}
	0.4	0.405377	1.11×10^{-16}	2.99×10^{-8}	4.41×10^{-3}
	0.6	0.389043	0	2.25×10^{-8}	4.04×10^{-3}
	0.8	0.372471	0	8.17×10^{-9}	3.68×10^{-3}
	1.0	0.355657	0	1.31×10^{-8}	3.33×10^{-3}

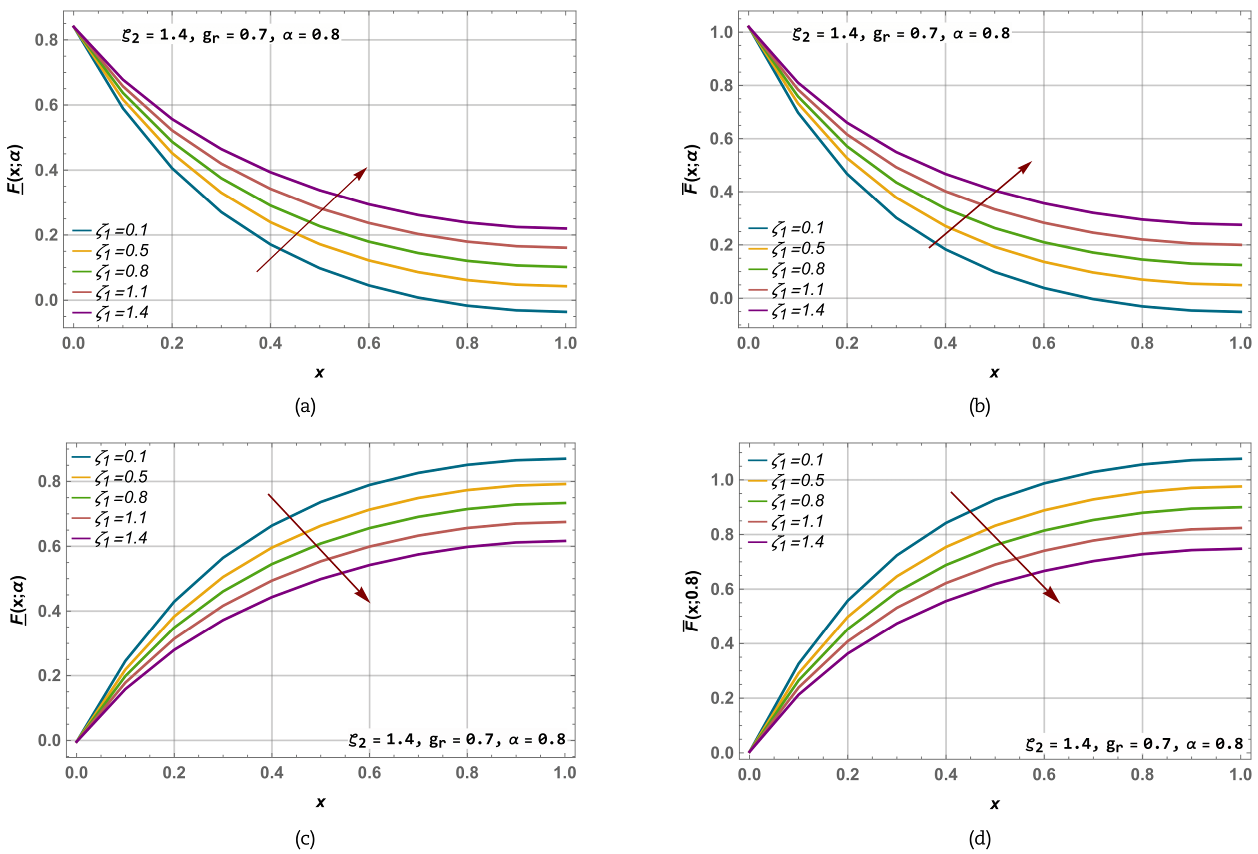

Fig. 2. Influence of ζ_1 on fuzzy velocity profile, (a) lower band of lifting case, (b) upper band of lifting case, (c) lower band of draining case, (d) upper band of draining case.

Similarly, Tables 5 to 7 also represent the fuzzy solutions at different values of ζ_1, ζ_2 and g_r keeping fuzzy parameter α with corresponding errors in lifting and drainage cases, respectively. Whereas Tables 8 to 11 demonstrate the fuzzy solution and absolute errors along nanoparticle volume fraction parameter α, influenced by fluid parameters ζ_2 and g_r for lifting and drainage case, respectively. The errors are evaluated using three algorithms namely Runge-Kutta Fehlberg, Crank-Nicolson, and modified homotopy perturbation to validate and analyze solutions.

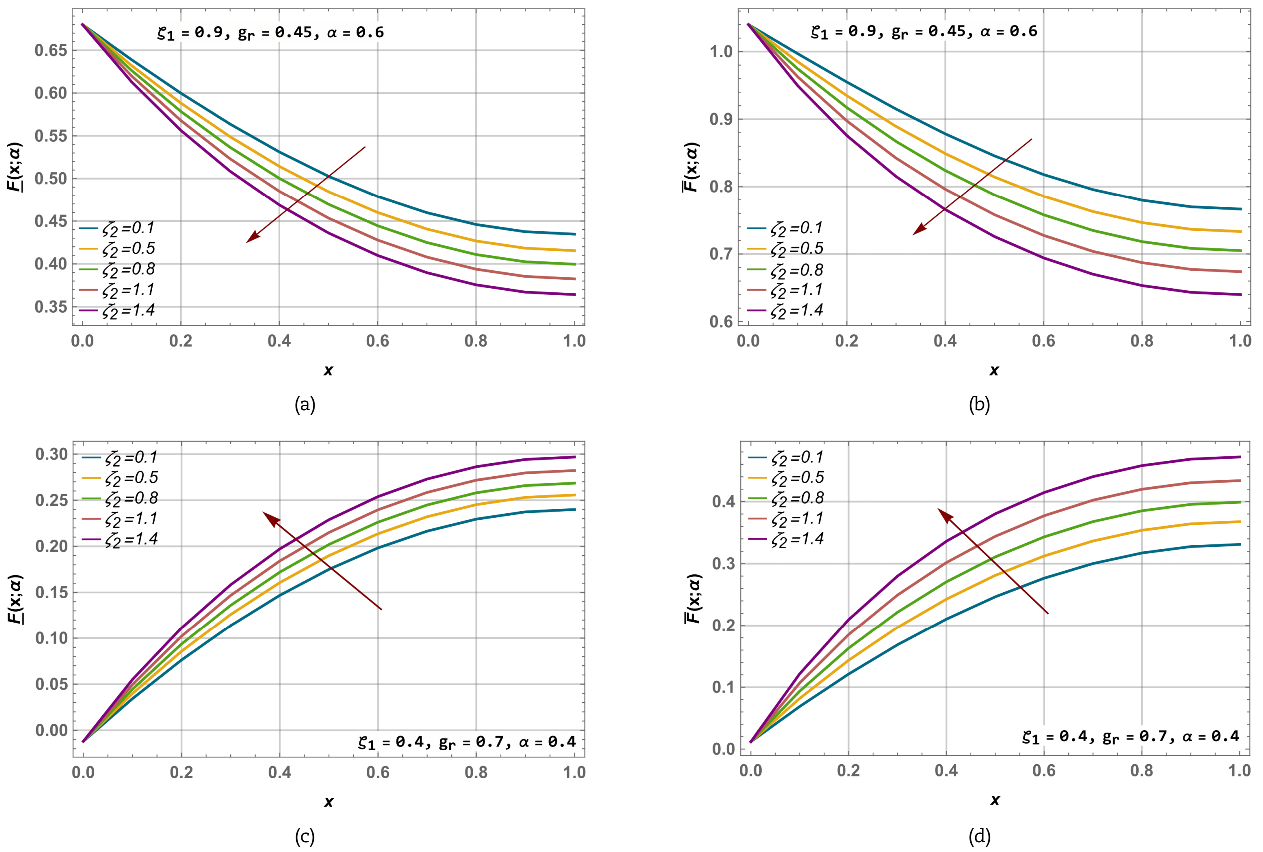

Fig. 3. Influence of ζ_2 on fuzzy velocity profile, (a) lower band of lifting case, (b) upper band of lifting case, (c) lower band of draining case, (d) upper band of draining case.

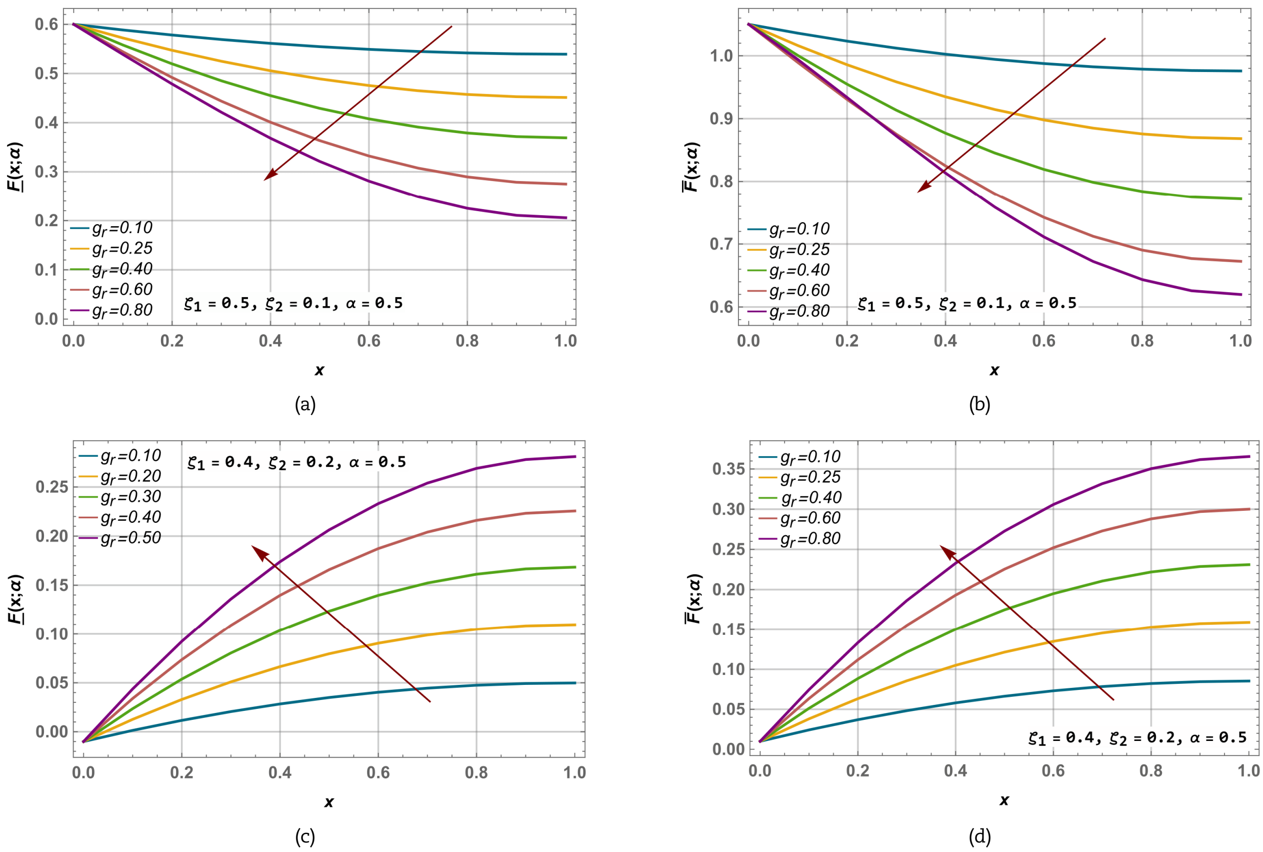

Fig. 4. Influence of g_r on fuzzy velocity profile, (a) lower band of lifting case, (b) upper band of lifting case, (c) lower band of draining case, (d) upper band of draining case.

Furthermore, the graphical investigation of how these parameters affect the fuzzy profile is carried out for both lifting and drainage cases. The material parameters ζ_1 and ζ_2 have distinct physical meanings in industrial usage. Specifically, ζ_1 is associated with the relaxation time of the polymer molecules in the fluid while ζ_2 represents the retardation time. When ζ_1 is increased, the fluid becomes more viscous and resistant to deformation. As a result, it flows more slowly. Conversely, when ζ_2 is increased, the flow behavior resembles shear thinning flow with least resistance to deform. As a consequence, it is able to flow more easily. Therefore, changes in values of ζ_1 and ζ_2 have a significant impact on the fluid behavior. By manipulating these parameters, it is possible to control the flow properties of the fluid and to optimize its performance for various applications. Figure 2 illustrates the variation in material parameter ζ_1. As shown in Figs. 2(a) and 2(b), an increase in material parameter ζ_1 enhances the lower and upper velocity profile in lifting case, while Figs. 2(c) and 2(d) depict a decrease in solution profile in drainage case.

On the other hand, in Fig. 3, the fuzzy velocity profile decreases as the material parameter ζ_2 increases in lifting case, whereas in draining case it behaves in-contrast. Figure 4 presents the impact of gravitational parameter g_r which is used for the effects of gravity on the fluid flow. This parameter represents the ratio of gravitational force to viscous forces and can affect the fluid velocity and film thickness. The observed behavior suggests that increase in the gravitational parameter leads to decease fuzzy solution in lifting case, where the fluid is being lifted against gravity. On the other hand, where the fluid flows downhill under the influence of gravity, an increase in the gravitational parameter also increases fuzzy solution.

Figures 5 and 6 provide graphical representations of the impact of fluid parameters ζ_1, ζ_2 and g_r on the fuzzified parameter α (nanoparticles volume fraction) for both lifting and drainage cases, respectively. The nanoparticle volume fraction parameter α describes the concentration of nanoparticles in the fluid. An increase in α can lead to changes in the rheological properties of the fluid, such as viscosity and shear stress. The nanoparticle concentration can also affect the stability of the fluid film on the moving belt, which is important in industrial processes such as coating and printing. In Fig. 5, the analysis shows the increase in fuzzy profile by increasing material parameter ζ_1 while the decline in fuzzy solution is observed for material parameter ζ_2 and gravitational parameter g_r. In contrast, in Fig. 6, fuzzy profile is decreasing along α by increasing ζ_1 and inverse relationship is observed for parameters ζ_2 and g_r. Given that fuzzy profiles are an extension of crisp profiles, it has been observed that the results of crisp solutions tend to lie at the midpoint of the solution bounds. In addition, the fuzzy solution remains consistent for both the upper and lower bounds when $\alpha = 1$. This suggests that the fuzzy solution is more robust and reliable than the crisp solution, as it takes into account a wider range of possibilities and can handle uncertainty better.

The illustration in Figs. 7 and 8 showcase a comparison between gold, alumina, and silver for both cases along the x-axis and fuzzified parameter α, respectively. Figure 9 presents the effect of the fractional parameter β along the $\alpha-$cut, where the fuzzy profile decreases as β increases in the lifting case. On the other hand, Fig. 10 shows the drainage case, where the lower bound is observed to decrease while the upper bound increases as β increases. Our work's uniqueness lies in its ability to capture the uncertain and imprecise rheological properties of complex fluids, which are not well-represented by traditional mathematical models, thus making it an essential tool for diverse applications in fields such as materials science, chemical engineering, and biomedical engineering.

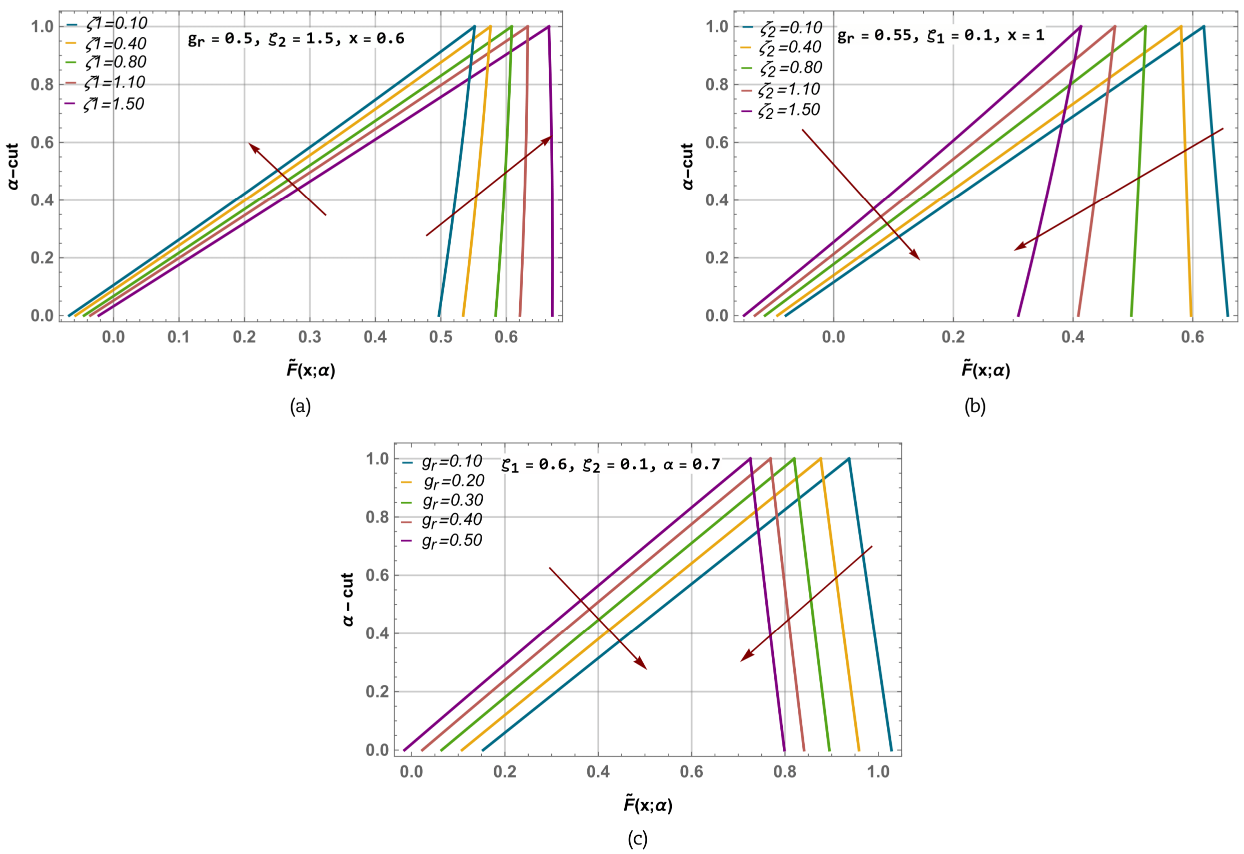

Fig. 5. Influence of different parameters on fuzzy velocity profile (lifting case), (a) influence of ζ_1, (b) influence of ζ_2, (c) influence of g_r.

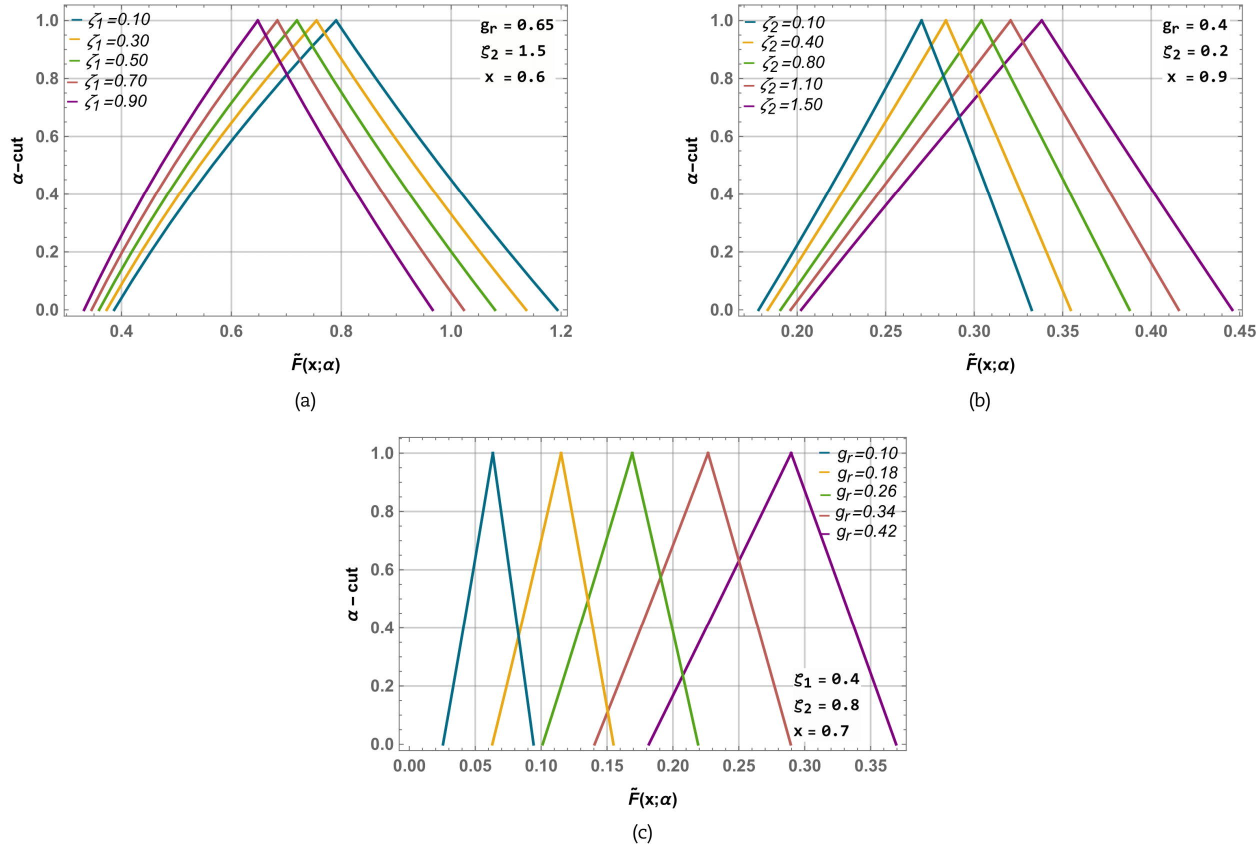

Fig. 6. Influence of different parameters on fuzzy velocity profile (draining case), (a) influence of ζ_1, (b) influence of ζ_2, (c) influence of g_r.

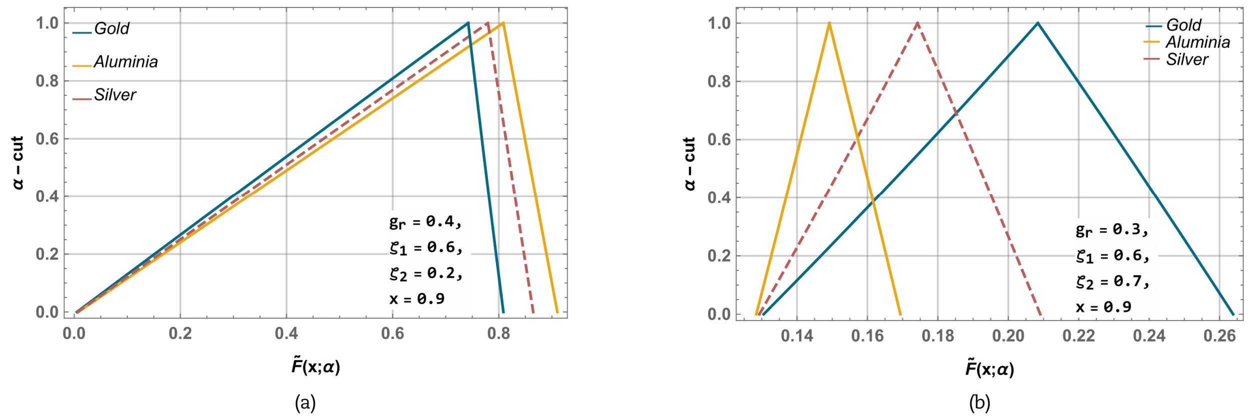

Fig. 7. Comparison of gold, alumina and silver, (a) lifting case, (b) draining case.

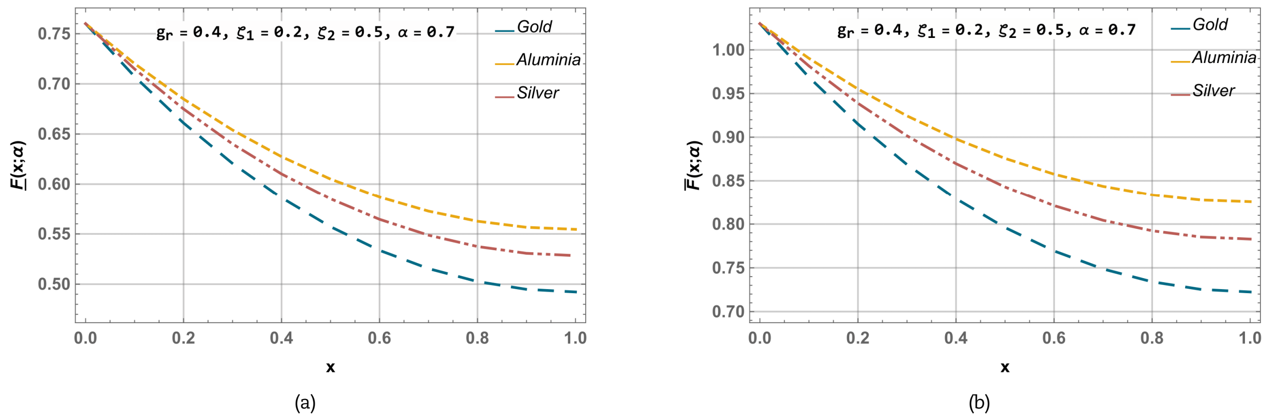

Fig. 8. Comparison of gold, alumina and silver, (a) lifting case, (b) draining case.

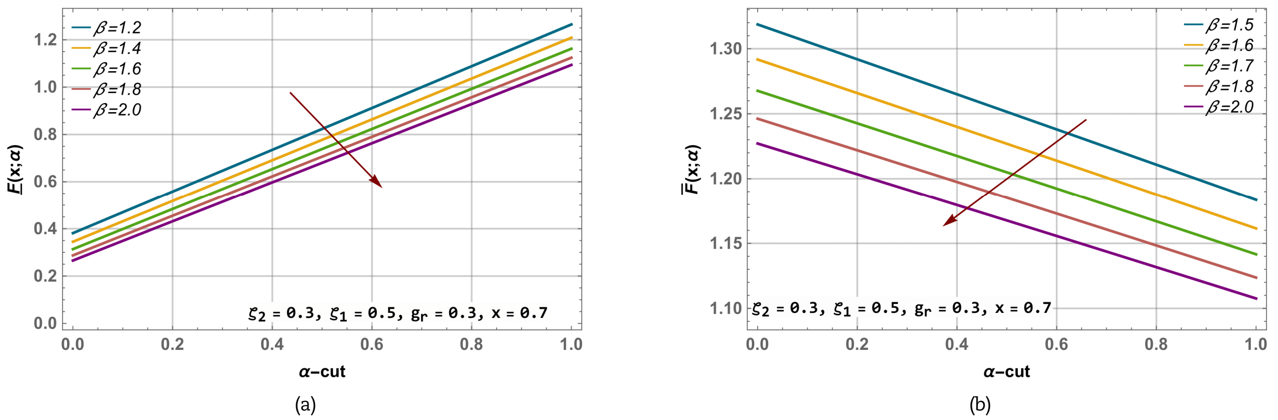

Fig. 9. Influence of fractional parameter β along membership function α in lifting case, (a) lower bound solution, (b) upper bound solution.

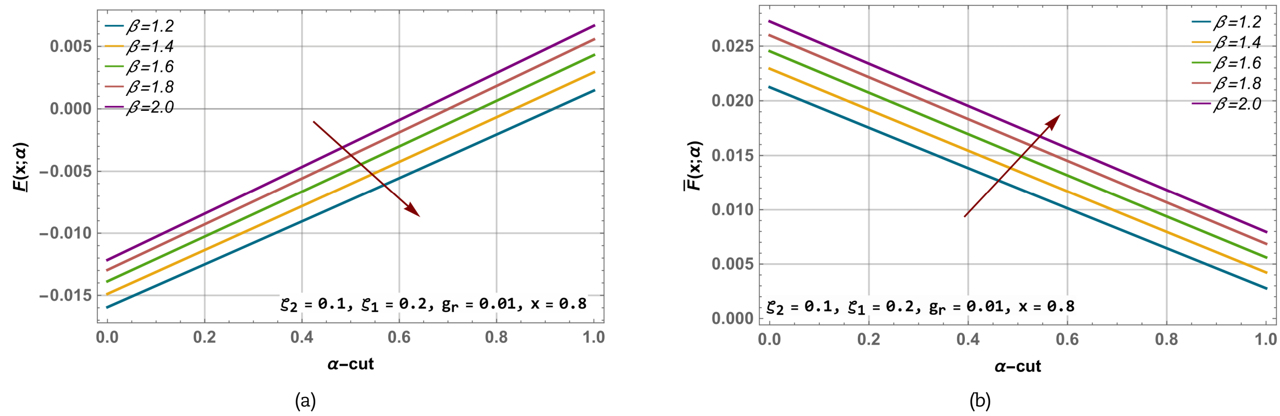

Fig. 10. Influence of fractional parameter β along membership function α in draining case, (a) lower bound solution, (b) upper bound solution.

7. Conclusion

The objective of the manuscript was to model and analyze thin film flow of fuzzy-fractional Oldroyd 6-constant nanofluid over a vertical belt in lifting and draining scenarios. Uncertainty in the current model was incorporated through $\alpha-$cut approach to develop triangular fuzzy numbers (TFNs). These TFNs were used in nanoparticle volume fraction and boundary conditions to completely fuzzified the modeled equations. Different algorithms including Runge-Kutta Fehlberg, Crank-Nikcolson and modified homotopy perturbation were used to validate and analyze the obtained fluid model. Firstly, we converted the obtained equations to highly nonlinear fuzzy differential systems. After solving these systems, the impact of different parameters (including fluid and fuzzy parameters) on the velocity field was observed numerically and graphically. Analysis revealed the following significant outcomes:

- The fuzzy velocity declined as the material parameter ζ_1 increases in draining case. On the other hand, inverse behavior is observed in lifting case.
- For the material parameter ζ_2 and gravitational parameter g_r, fuzzy velocity field boosted up in drainage case whereas inverse relationship is seen in lifting case.
- Material parameter ζ_1 increases nanofluid velocity at both upper and lower bound, whereas parameters ζ_2 and g_r decreases the velocity profile at both bounds in case of lifting. On the other hand, inverse relationship is seen in drainage case.
- Fractional parameter β shows decrease in fuzzy velocity profile in the lifting case. But in draining case, velocity profile show decline at lower bound while increase is observed at upper bound.
- The relationship between fuzzy and crisp profiles indicated that the results of crisp solutions tended to fall within the solution bounds which is the validation of obtained solutions as fuzzy profile is the extension of crisp profile.
- At $\alpha = 1$, the fuzzy solution remained the same for both upper and lower bounds.
- The findings of this study can have potential applications in various industries such as coating, printing, and food processing. Further research on fuzzy-fractional differential equations can enhance the understanding of complex phenomena.

Author Contributions

The authors confirmed the contributions to this article as follows: M. Qayyum: Conceptualization; Supervision; Methodology; Analysis; Validation; Writing, Review and Editing. A. Tahir: Code Writing; Methodology; Visualization; Validation; Writing Original Draft. S.T. Saeed: Analysis; validation; Writing, review and editing of manuscript; Software. The manuscript was written through the contribution of all authors. All authors discussed the results, reviewed, and approved the final version of the manuscript.

Acknowledgments

The authors are highly thankful and grateful for support of this research article.

Conflict of Interest

The authors declared no potential conflicts of interest concerning the research, authorship, and publication of this article.

Funding

The authors received no financial support for the research, authorship, and publication of this article.

Data Availability Statements

The research is not associated with any data.

References

[1] Fetecau, C., Fetecau, C., Vieru, D., On some helical flows of oldroyd-b fluids, *Acta Mechanica*, 189(1-4), 2006, 53–63.
[2] Dunn, J.E., Rajagopal, K.R., Fluids of differential type: Critical review and thermodynamic analysis, *International Journal of Engineering Science*, 33(5), 1995, 689–729.
[3] Ohayon, D., Nikiforidis, G., Savva, A., Giugni, A., Wustoni, S., Palanisamy, T., Chen, X., Maria, I.P., Fabrizio, E.D., Costa, P.M.F.J., Biofuel powered glucose detection in bodily fluids with an n-type conjugated polymer, *Nature Materials*, 19(4), 2020, 456–463.
[4] Hayat, T., Siddiqui, A.M., Asghar, S., Some simple flows of an oldroyd-b fluid, *International Journal of Engineering Science*, 39(2), 2001, 135–147.
[5] Rajagopal, K.R., On an exact solution for the flow of an oldroyd-b fluid, *Istanbul Teknik Üniversitesi Bülteni*, 49, 1996, 617–624.
[6] Pontrelli, G., Longitudinal and torsional oscillations of a rod in an oldroyd-b fluid with suction or injection, *Acta Mechanica*, 123(1-4), 1997, 57–68.
[7] Riaz, M.B., Rehman, A.U., Wojciechowski, A., Atangana, A., Heat and mass flux analysis of magneto-free convection flow of oldroyd-b fluid through porous layered inclined plate, *Scientific Reports*, 13(1), 2023, 1–15.
[8] Hayat, T., Khan, M., Asghar, S., Homotopy analysis of mhd flows of an oldroyd 8-constant fluid, *Acta Mechanica*, 168(3-4), 2004, 213–232.
[9] Soumya, D.O., Venkatesh, P., Gireesha, B.J., Gombi, M.R., Krishnamurthy, K.R., Flow and thermal analysis of oldroyd 8 constant fluid in a porous channel, *Heat Transfer*, 52(2), 2023, 1413–1432.
[10] Saengow, C., Giacomin, A.J., Kolitawong, C., Exact analytical solution for large-amplitude oscillatory shear flow from oldroyd 8-constant framework: Shear stress, *Physics of Fluids*, 29(4), 2017, 043101.
[11] Saengow, C., Giacomin, A.J., Grizzuti, N., Pasquino, R., Startup steady shear flow from the oldroyd 8-constant framework, *Physics of Fluids*, 31(6), 2019, 063101.
[12] Baris, S., Flow of an oldroyd 6-constant fluid between intersecting planes, one of which is moving, *Acta Mechanica*, 147(1-4), 2001, 125–135.
[13] Wang, Y., Hayat, T., Hutter, K., On non-linear magnetohydrodynamic problems of an oldroyd 6-constant fluid, *International Journal of Non-Linear Mechanics*, 40(1), 2005, 49–58.
[14] Manzoor, T., Iqbal, S., Shah, M.A., A note on the slip effects of an oldroyd 6-constant fluid: Optimal homotopy asymptotic method, *Frontiers in Physics*, 10, 2022, 1003000.
[15] Rana, M.A., Siddiqui, A.M., Qamar, R., Hall effects on hydromagnetic flow of an oldroyd 6-constant fluid between concentric cylinders, *Chaos, Solitons and Fractals*, 39(1), 2009, 204–213.
[16] Qayyum, M., Fatima, Q., Analysis of thin film flows of pseudo-plastic and oldroyd 6-constant fluids using modified residual power series algorithm, *Journal of the Indian Chemical Society*, 99(11), 2022, 100755.
[17] Bhatti, M.M., Michaelides, E.E., Oldroyd 6-constant electro-magneto-hydrodynamic fluid flow through parallel micro-plates with heat transfer using darcy-brinkman-forchheimer model: A parametric investigation, *Mathematics in Engineering*, 5(3), 2023, 1–19.
[18] Salawu, S.O., Disu, A.B., Branch-chain criticality and thermal explosion of oldroyd 6-constant fluid for a generalized couette reactive flow, *South African Journal of Chemical Engineering*, 34, 2020, 90–96.
[19] Qayyum, M., Shah, S.I.A., Yao, S.W., Imran, N., Sohail, M., et al., Homotopic fractional analysis of thin film flow of oldroyd 6-constant fluid, *Alexandria Engineering Journal*, 60(6), 2021, 5311–5322.
[20] Zadeh, L.A., Fuzzy sets, *Information and Control*, 8(3), 1965, 338–353.
[21] Pedro, F.S., Barros, L.C.D., Esmi, E., Population growth model via interactive fuzzy differential equation, *Information Sciences*, 481, 2019, 160–173.
[22] Naschie, M.S.E., From experimental quantum optics to quantum gravity via a fuzzy kahler manifold, *Chaos, Solitons and Fractals*, 25(5), 2005, 969–977.
[23] Barro, S., Mar, R., *Fuzzy Logic in Medicine*, Physica-Verlag, 2002.
[24] Nadeem, M., Siddique, I., Jarad, F., Jamil, R.N., Numerical study of MHD third-grade fluid flow through an inclined channel with ohmic heating under fuzzy environment, *Mathematical Problems in Engineering*, 2021, 1–17.
[25] Qayyum, M., Tahir, A., Saeed, S.T., Akgul, A., Series-form solutions of generalized fractional-fisher models with uncertainties using hybrid approach in caputo sense, *Chaos, Solitons and Fractals*, 172, 2023, 113502.
[26] Qayyum, M., Tahir, A., Acharya, S., et al., New solutions of fuzzy-fractional fisher models via optimal he–laplace algorithm, *International Journal of Intelligent Systems*, 2023, https://doi.org/10.1155/2023/7084316.
[27] Khaliq, R., Iqbal, P., Bhat, S.A., Sheergojri, A.R., A fuzzy mathematical model for tumor growth pattern using generalized hukuhara derivative and its numerical analysis, *Applied Soft Computing*, 118, 2022, 108467.
[28] Naeem, M., Rezazadeh, H., Khammash, A.A., Shah, R., Zaland, S., Analysis of the fuzzy fractional-order solitary wave solutions for the KdV equation in the sense of caputo-fabrizio derivative, *Journal of Mathematics*, 2022, 1–12.
[29] Hoa, N.V., Vu, H., Duc, T.M., Fuzzy fractional differential equations under caputo–katugampola fractional derivative approach, *Fuzzy Sets and Systems*, 375, 2019, 70–99.
[30] Rashid, S., Kaabar, M.K.A., Althobaiti, A., Alqurashi, M.S., Constructing analytical estimates of the fuzzy fractional order boussinesq model and their application in oceanography, *Journal of Ocean Engineering and Science*, 8(2), 2023, 196–215.
[31] Akram, M., Muhammad, G., Allahviranloo, T., Ali, G., A solving method for two-dimensional homogeneous system of fuzzy fractional differential equations, *AIMS Mathematics*, 8, 2023, 228–263.
[32] Sivashankar, M., Sabarinathan, S., Govindan, V., Gamiz, U.F., Noeiaghdam, S., Stability analysis of covid-19 outbreak using caputo-fabrizio fractional differential equation, *AIMS Mathematics*, 8(2), 2023, 2720–2735.
[33] Sohrabi, M., Zandieh, M., Shokouhifar, M., Sustainable inventory management in blood banks considering health equity using a combined metaheuristic-based robust fuzzy stochastic programming, *Socio-Economic Planning Sciences*, 86, 2023, 101462.
[34] Mondal, D., Garai, T., Roy, G.C., Alam, S.U., Application of a fuzzy differential equation system to the oil and gas industry safety model, *International Journal of Information Technology*, 15, 2023, 1243–1253.
[35] Gani, A.N., Assarudeen, S.N.M., A new operation on triangular fuzzy number for solving fuzzy linear programming problem, *Applied Mathematical Sciences*, 6(11), 2012, 525–532.
[36] Pathinathan, T., Ponnivalavan, K., Dison, E.M., Different types of fuzzy numbers and certain properties, *Journal of Computer and Mathematical Sciences*, 6(11), 2015, 631–651.

[37] Gasilov, N., Amrahov, S.G., Fatullayev, A.G., A geometric approach to solve fuzzy linear systems of differential equations, *arXiv preprint arXiv:0910.4307*, 2009.
[38] Tuan, N.H., Mohammadi, H., Rezapour, S., A mathematical model for COVID-19 transmission by using the caputo fractional derivative, *Chaos, Solitons & Fractals*, 140, 2020, 110107.

ORCID iD

Mubashir Qayyum https://orcid.org/0000-0002-6701-5640
Aneeza Tahir https://orcid.org/0009-0005-5618-0906
Syed Tauseef Saeed https://orcid.org/0009-0001-4221-052X

How to cite this article: Qayyum M., Tahir A., Saeed S.T. Modeling and Numerical Simulations of Fuzzy-Fractional Oldroyd 6-Constant Nanofluid, *J. Appl. Comput. Mech.*, 11(2), 2025, 485-501. https://doi.org/10.22055/jacm.2024.46976.4637